OXYGEN ISOTOPE ANALYSIS IN TREE-RINGS OF PTEROCAROUS ANGOLENSIS GROWING IN ZIMBABWE

by

Kerry Elizabeth McLeran

B.A., University of Nevada, 2010

A Thesis
Submitted in Partial Fulfillment of the Requirements for the
Master of Science.

Department of Geography & Environmental Resources
in the Graduate School
Southern Illinois University Carbondale
May 2013

THESIS APPROVAL

OXYGEN ISOTOPE ANALYSIS IN TREE-RINGS OF PTEROCAROUS ANGOLENSIS GROWING IN ZIMBABWE

By

Kerry Elizabeth McLeran

A Thesis Submitted in Partial

Fulfillment of the Requirements

for the Degree of

Master of Science

in the field of Geography & Environmental Resources

Approved by:

Dr. Justin Schoof, Chair

Dr. Matthew Therrell

Dr. Liliana Lefticariu

Dr. Justin Schoof

Graduate School
Southern Illinois University Carbondale
April 3rd 2013

AN ABSTRACT OF THE THESIS OF

KERRY ELIZABETH MCLERAN, for the Master's of Science degree in GEOGRAPHY & ENVIRONMENTAL RESOURCES, presented on April 3, 2013, at Southern Illinois University Carbondale.

TITLE: OXYGEN ISOTOPE ANALYSIS IN TREE-RINGS OF PTEROCAROUS ANGOLENSIS GROWING IN ZIMBABWE

MAJOR PROFESSOR: Dr. Matthew Therrell

My study was designed to identify the relationships between climate variables, such as precipitation and temperature, and $\delta^{18}O$ values of tree ring α-cellulose extracted from exactly dated tree rings of *Pterocarpus angolensis* growing in the arid to semiarid Mzola region of western Zimbabwe. This species is known to be sensitive to seasonal variation in rainfall. In this region, the wet season occurs during the austral summer from mid November to early April followed by a dry winter season from around June through October. Overall, the total annual rainfall exhibits a high degree of spatial and temporal variation with a mean of less than 600 mm per year. I applied the Modified Brendel technique to isolate α-cellulose from raw wood samples extracted from two *P. angolensis* trees and measured the α-cellulose $\delta^{18}O$ values using continuous flow isotope ratio mass spectrometry. I developed a 30-year (1955-1984) α-cellulose $\delta^{18}O$ chronology and correlated it with tree-ring width, meteoric water $\delta^{18}O$ values, monthly and seasonal precipitation totals, and mean seasonal temperature. The $\delta^{18}O$ values of meteoric water for this region were obtained from the Global Network of Isotopes in Precipitation (GNIP) and correlated with the $\delta^{18}O$

values of tree ring α-cellulose. The strongest correlations were observed between α-cellulose $\delta^{18}O$ values and February total precipitation ($r = -0.49$, $p = 0.006$) and to a lesser degree total wet season (NDJFMA) precipitation, In particular, unusually rainy wet seasons were significantly correlated ($r = -0.79$, $P = 0.007$) with α-cellulose $\delta^{18}O$. This relationship is consistent with ^{18}O-depleted values measured in summer precipitation during periods of high rainfall, which is most likely the result of the isotopic amount effect reported in tropical regions. I also identified a positive correlation ($r = 0.49$, $p = 0.03$) between alpha-cellulose $\delta^{18}O$ and the $\delta^{18}O$ values of meteoric water, and investigated the possibility of an isotopic temperature effect for $\delta^{18}O$ in meteoric water, which also may be reflected in the $\delta^{18}O$ values in tree ring α-cellulose. The strongest correlation with mean temperature was observed during the wet summer season ($r = 0.56$, $p = 0.01$). My results suggest that the $\delta^{18}O$ values of *P. angolensis* tree rings can be used as natural indicators of paleoclimate in southern Africa.

DEDICATION

I dedicate this project to Dr. Gary Hausladen of the University of Nevada, Reno.

ACKNOWLEDGMENTS

First and foremost, I would like to acknowledge Dr. Matthew Therrell for making this project possible. Thank you for your encouragement, support and guidance through this process. I would like to thank Dr. Liliana Lefticariu for sharing her expertise of isotope geochemistry and for allowing me access to her Geochemistry Lab. I would like to thank Dr. Justin Schoof for his assistance with the statistical and climatological portions of my research. I couldn't have asked for a better Thesis committee.

I would also like to thank Dr. Mihai Lefticariu of the Isotope Ratio Mass Spectrometry Facility for all his time and effort in analyzing my samples and Bill Huggett for allowing me open access to the Coal Research Lab.

Lastly, I would like to thank my parents for their love, support, and encouragement throughout this process.

TABLE OF CONTENTS

LIST OF TABLES

LIST OF FIGURES

FIGURE PAGE

CHAPTER 1

INTRODUCTION

1.1 Background

The climate in southern Africa is highly variable, with large fluctuations in precipitation on both temporal and spatial scales, which leaves the region vulnerable to severe droughts and floods (Usman and Reason, 2004). Inter- and intra-annual variability in precipitation are considered key climatic elements that determine the success of agriculture, the largest business sector in southern Africa (Leichenko and O'Brien, 2001). The majority of the population in southern Africa struggles from poor infrastructure and low socio-economic development, and extreme weather events and climate anomalies can be devastating to both people and property (Fauchereau et al., 2003). In Zimbabwe, approximately 90% of the country's population inhabits rural areas and relies on rain-fed, subsistence agriculture, typically cultivating small-scale holdings of 0.2–3 ha (Ellis et al., 2003; Stringer et al., 2009), with maize constituting the staple crop. Total internal renewable water resources in Zimbabwe are estimated to be 12-14 km^3/year, of which more than 11 km^3 are surface water resources. Agriculture is the greatest water consumer accounting for 79 percent of total water use (Nkomozepi and Chung, 2012). Extended droughts during the 1982-1983 and 1991-1992 summer seasons led to devastating crop failure over much of southern Africa, emphasizing just how vulnerable the region's food security and water resources are to climate extremes (Hulme et al., 1996; Fauchereau et al., 2003). During the drought of 1992 in southern Africa, total cereal production was cut nearly in half, and by nearly one-third during the drought in 1995 (Leichenko and O'Brien, 2001). In February of 2000, severe flooding in northern Mozambique, South Africa,

and Zimbabwe killed 600 people, displaced hundreds of thousands more, and destroyed 200 bridges and 1000 km of roadway (Dyson and van Heerden, 2001; Fauchereau et al., 2003).

The annual occurrence of wet and dry seasons in southern Africa is driven by changes in the location of the Intertropical Convergence Zone (ITCZ). The ITCZ reaches its northernmost position (about 15°N) in May and then migrates south to its southernmost position (about 5°S) in December (Nicholson, 1981). Variations in precipitation over southern Africa occur at roughly 2.3, 3.5, and 5-year cycles, which is the same resolution of the El Niño Southern Oscillation (ENSO) phenomenon, suggesting a direct relationship between global processes and precipitation variability over southern Africa (Nicholson, 1989). Typically, dry conditions occur over much of southern Africa during ENSO events, especially during the months of February to May, while above-normal precipitation occurs during La Niña events (Unganai, 1996; Nicholson, 2001).

Changes in the natural variability of earth's climate system due to anthropogenic modifications of the composition of the atmosphere are correlated with natural disasters, such as droughts, in southern Africa. The Intergovernmental Panel on Climate Change (IPCC) predicts that the impacts of drought will become more severe as a result of global climate change and, owing to its great impact on human activities, future variability in precipitation deserves much attention. Precipitation extremes typically have a greater affect on human activity than slight changes in mean precipitation, which warrants analysis of extreme behavior under changing climatic conditions.

Several general circulation models (GCMs) indicate future warming across southern Africa ranging from 0.2°C per decade (low scenario) to more than 0.5°C per decade (high scenario) (UNEP, 2009). GCMs have revealed a warming trend in Zimbabwe (in both minimum and maximum temperatures) since at least 1897, with a maximum increase of 1.2°C found during

austral winter (Unganai, 1996). Hulme et al. (2001) identified an increase in mean annual diurnal temperature (almost entirely due to increases in the November-February wet season temperatures) in Zimbabwe of 0.5°C to 1°C since the 1950s. Zimbabwe has been drier in the last few decades and GCMs have identified a declining trend in precipitation during the DJF and JFM seasons by about 10 and 16 percent, respectively (Unganai, 1996). Utilizing an ensemble of GCMs, Shongwe et al., (2009) identified an increase in the severity of dry extremes and statistically significant decreases in mean precipitation during the wet season over western southern Africa. The beginning of the wet season has been notably delayed while the duration of the season is decreasing throughout most of the region.

1.2 Statement of Problem

Instrumental weather records in southern Africa are largely limited to the last 100 years and documentary weather-related data is difficult to find prior to the 1800s, which is why the spatial variability of precipitation has been studied in other parts of the world, but few studies for Africa and even fewer for southern Africa (Verschuren, 2004). One possible way to mitigate the future impacts associated with precipitation variability in southern Africa is to establish a better understanding of natural and/or anthropogenic factors that influence climate variability over this region. Examining tree-rings can provide opportunities for reconstructing past climate (e.g. Fichtler et al., 2004; Therrell et al., 2006; Le Quesne et al., 2006; Liang et al., 2008; Li et al., 2006). Ring-width analysis has a unique advantage among the proxies used in paleoclimate analysis (e.g., corals, ice cores, lake sediments, pollen, speleothems) because they: are widely distributed, maintain a continuous record, and are annually resolved (Managave and Ramesh, 2011). Besides identifying a tree's age, tree-rings can often provide insight into the climate of the

area in which the tree grew based on different variables (e.g., precipitation and temperature) that contribute to the growth of each annual ring, such as precipitation and temperature. Investigating variations in these factors allows scientists to understand climate variability as well as determine past environmental conditions.

Measuring stable isotope ratios (commonly oxygen, carbon, and hydrogen) from tree-rings has brought about additional critical understanding of past climatic conditions. Isotope signals in tree rings allow for long chronologies, high resolution, and statistically defined confidence intervals (McCarroll and Loader, 2004). Furthermore, some research has suggested that ring-width is influenced more by biological and ecological factors than is stable isotope composition (Managave and Ramesh, 2011) and by incorporating stable isotope analysis into ring-width paleoclimate studies, some of the issues that arise when using only ring-width analysis may be avoided.

1.3 Southern Africa Proxy Paleoclimate Reconstructions

Patterns of considerable climatic change in southern Africa over the past 10,000 years at millennial, interdecadal, and decadal timescales have been inferred from a handful of climate proxies (Brook et al., 1999; Holmgren et al., 2001; Lee-Thorp et al., 2001; Thompson et al., 2002; Therrell et al., 2006; Zinke et al., 2009; Grove et al., 2012). Climate reconstructions based on the ^{18}O and ^{13}C values of a uranium-dated stalagmite, from Cold Air Cave in north-eastern South Africa, suggests that precipitation and temperature fluctuated greatly and quickly over the last ~6,500 years on centennial and multi-decadal timescales (Lee-Thorp et al., 2001). Lake level reconstructions of Lake Malawi and Lake Chilwa in Malawi revealed that intermediate lake levels occurred in the 1880s and the 1950s-1960s, pronounced lowstand levels occurred during the 1900s and 1910s, and a recovery to peak levels has been occurring since the 1960s (Verschuren, 2004).

The fluctuations in lake levels were large in magnitude, with most of the fluctuations being at least five to 10 m (Nicholson, 2000). Wet season precipitation increased during the mid Holocene warm phase, followed by a pronounced cool and dry period ~3,200 years ago, culminating around the 1750s. The first and currently only tree-ring reconstruction of precipitation in tropical Africa used a 200-year regional chronology based on samples of *P. angolensis* from Zimbabwe (Therrell et al., 2006). The reconstruction indicates seven consecutive years of drought conditions from 1882 to 1888 that were followed by six consecutive years of high precipitation between 1897 and 1902. The reconstruction further suggests that a ten-year drought between 1859 and 1868 may have exceeded similar events in the modern observational record. An eight-year drought occurred between 1989 and 1995, which surpassed the 1882 – 1888 drought (annual mean precipitation = 418 mm vs. a mean of 452 mm). The reconstruction also shows that drought conditions occurred in the 1820s and 1840s as well as a wet period in the 1830s (Therrell et al., 2006). Rainfall reconstructions from two subtropical western Indian Ocean coral oxygen isotope chronologies suggest that rainfall over southern Africa is characterized by both multidecadal (30 years) and interdecadal fluctuations spanning from 16 to 20 years and interannual variability ranging from 2.9 to 3.6 years (Zinke et al., 2009). In their study of $\delta^{18}O$ in cellulose of *Breonadia salicina* (Matumi) trees growing in South Africa, Norstrom et al., (2008) analyzed the $\delta^{18}O$ cellulose values of two 600-year old *B. salicina* trees, lacking apparentannual growth rings, to test the isotope variations as a regional climate proxy. They determined that different factors, such as regional climate conditions and sight-specific factors associated with riparian growth environments, during the lifetime of the two trees dominated the $\delta^{18}O$ signal in the tree ring cellulose, thus complicating the possibilities of using the $\delta^{18}O$ cellulose series from this species for paleoclimate studies.

For my research, I investigated the relationship between oxygen isotopes in tree-ring alpha-cellulose ($\delta^{18}O_{\alpha c}$) of *Pterocarpus angolensis*, ring-width, temperature, monthly and seasonal precipitation variability, and the $\delta^{18}O$ values of meteoric water ($\delta^{18}O_{meteoric)}$ Zimbabwe, as well as seasonal sea surface temperatures in the tropics. This is the first isotope based climatic investigation for Zimbabwe and southern Africa based on the $\delta^{18}O_{\alpha c}$ values of annually dated tree-rings. The following questions are addressed by my research:

1. Do *Pterocarpus angolensis* trees growing in Zimbabwe record climate signals that can be identified by analyzing the $\delta^{18}O_{\alpha c}$ values of each ring?
2. Are ring-width and $\delta^{18}O_{\alpha c}$ values influenced by the same climate signals?

1.4 Study Area

Zimbabwe is located between latitude 15.5 and 22.5°S and longitude 25 and 33°E. Temperatures remain high and fairly constant throughout the year with a diurnal temperature range of about 10 to 15°C and an annual range that does not exceed 6°C. Annual mean temperatures range from 15°C in the highest elevations to above 25°C at low elevations (Unganai, 1996), with October being the warmest month and June and July the coolest. Mean annual precipitation ranges from 800 mm in the northeast down to 400 mm in the south. There is a wet season lasting from October to April and a dry season spanning May to September.

The partial cross-sections used in this study are from a previously reported collection of *P. angolensis* from the Mzola forest in northwestern Zimbabwe (Mushove et al., 1997). The Mzola forest is located in the arid to semi-arid Mzola region of western Zimbabwe (-18.20°, 27.40°, 1,106 meters asl; Fig. 1.1) Total annual rainfall exhibits a high degree of spatial and temporal variation

with a mean of ~600 mm per year (Food and Agriculture Organization; Fig. 1.2). Approximately 80% of annual precipitation occurs between November and February (~579 mm) and, during the dry season (June – October), average precipitation amount is ~24.4 mm.

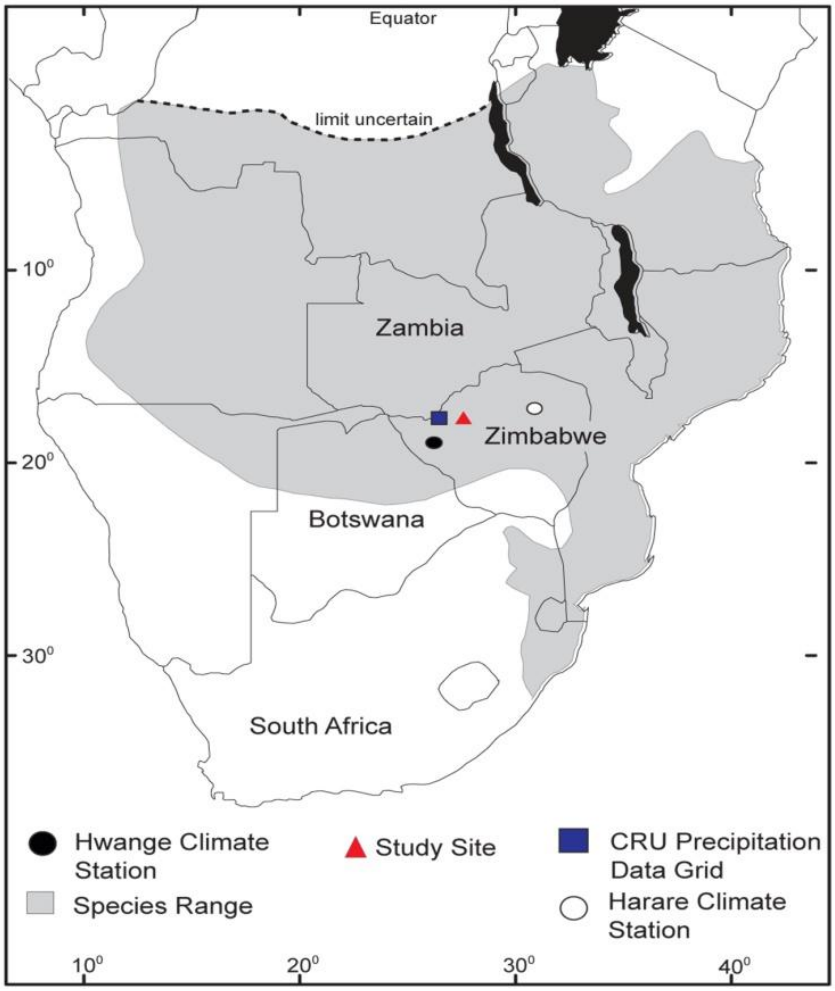

Figure 1.1 Location of the Mzola forest study site, climate stations and CRU grid in Zimbabwe (e.g., Therrell et al., 2006).

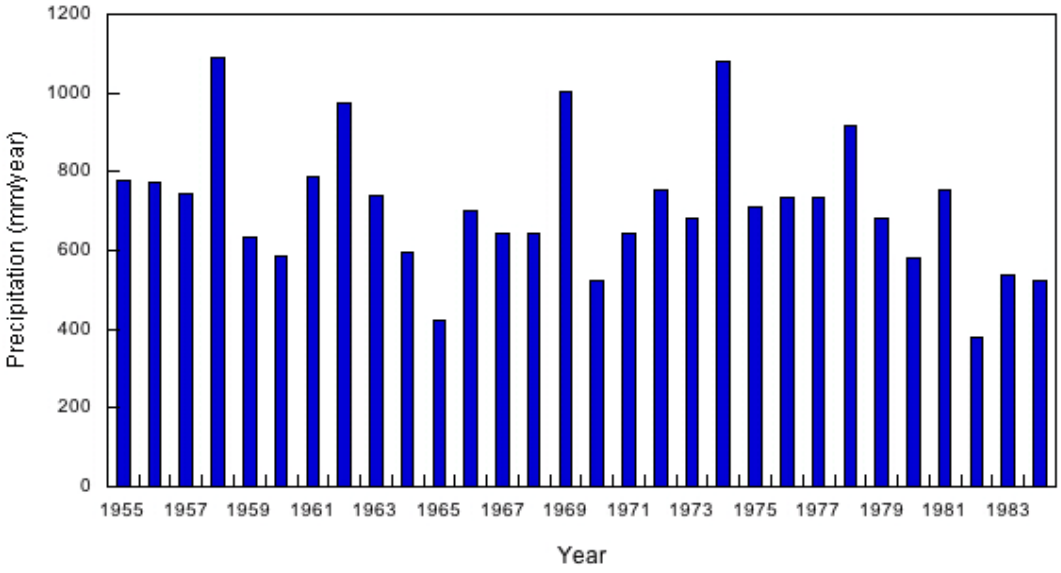

Figure 1.2 Annual (January to December) precipitation amount from the 17.5x26.5º CRU precipitation data grid.

1.5 *Pterocarpus Angolensis*

Pterocarpus angolensis (also known as Bloodwood, Kiaat, and Mukwa; Fig. 1.3) is a widely distributed, deciduous, canopy species found in savanna woodlands throughout Africa south of the equator (Fig. 1.4; Shackleton, 2002) and is one of the most valuable hardwood species in southern Africa. It comprises the largest volume of woodcarvings and furniture sold in this region (Shackleton and Adelfang, 1992). When environmental conditions are favorable, *P. angolensis* can grow up to 25 m in height and one meter in diameter. *P. angolensis* is restricted to dry subhumid climate zones, with a single rainy season, mean annual rainfall between 500-1,250 mm, and a temperature range of 20°C in the warmest month and 4°C in the coldest month (von Breitenbach, 1973).

Figure 1.3 A *Pterocarpus angolensis* growing in Zimbabwe. Source: M. Therrell (2009).

Figure 1.4 A savanna woodland in Zimbabwe. Source: M. Therrell (2009).

The root system of *P. angolensis* is extensive including a taproot (the main root of a plant growing downward from the stem) between ~ 46 and 90 cm in length. The phenology of *P. angolensis* strongly corresponds to the seasonality of precipitation. Flowering and leaf flush occur during the start of the rainy season in early October through to November. Mature leaves are visible between November and June and the distinctive circular seed pods are produced January to April. The leaves begin to change color between January and April, and by July, *P. angolensis* are leafless and will remain so until the end of the dry season (Shackleton, 2002). This dramatic seasonality in flowering, leaf flush, and leaf fall strongly suggest that radial growth is restricted to the summer wet season (Stahle et al., 1999).

1.6 Isotope Systematics

Each chemical element (e.g., Carbon, Nitrogen, Oxygen) has its own atomic number, which is equal to the number of protons in the atom's nucleus, and this is what determines the chemical properties of an atom of a particular element. Any oxygen atom has eight protons and therefore an atomic number of eight. The mass number of an atom is equal to the number of protons and neutrons in the nucleus. The number of neutrons in the nucleus can be calculated by subtracting the atomic number from the mass number.

An isotope is an atom of a particular element that has the same number of protons and electrons but differs in mass from other atoms of the same element due to differing numbers of neutrons in its nucleus (Fig. 1.5). The number of protons in the nucleus of an atom cannot change without altering the chemical properties of that atom, but the number of neutrons can vary without changing the element of a particular atom. For example, if an oxygen atom has eight protons in its nucleus (mass number), eight electrons in orbitals around the nucleus, and an atomic number of 16,

the number of neutrons in the nucleus of that oxygen atom is: 16 – 8 = 8. This means this atom is an ^{16}O isotope.

The two most abundant stable isotopes of oxygen are:

^{16}O → 8 protons and 8 neutrons (considered the "light" oxygen isotope)

^{18}O → 8 protons and 10 neutrons (considered the "heavy" oxygen isotope)

The differences in mass between these two oxygen isotopes results in slightly different bond strengths to other elements.

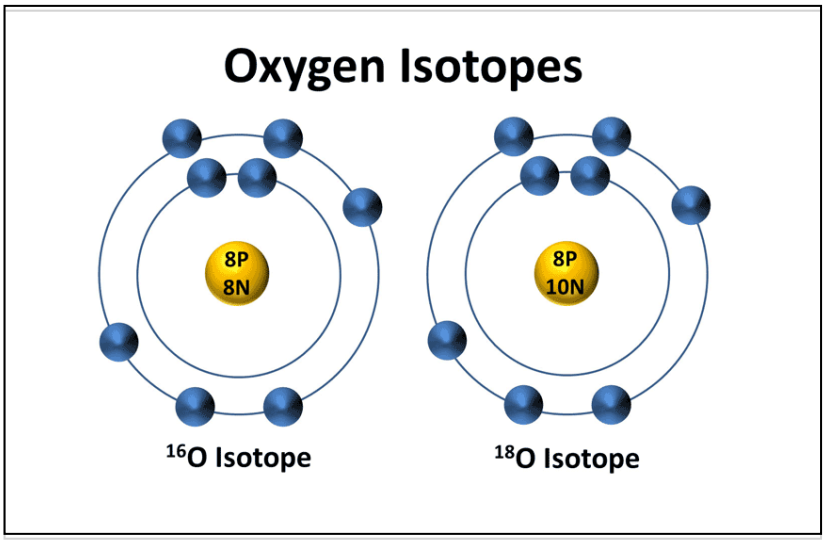

Figure 1.5 Oxygen-16 (^{16}O) and oxygen-18 (^{18}O) isotopes (NASA Paleoclimatology webpage; NASA CSI: South Florida page).

Isotope fractionation is the separation of isotopes between two or more substances and is measured as variations in the isotopic ratio (e.g., $^{18}O/^{16}O$) due to a chemical or physical process and is proportional to the relative mass difference between two isotopes (e.g., ^{16}O and ^{18}O). The fractionation factors are strongly dependent on temperature (Managave, 2011). Equilibrium isotope fractionation occurs when two or more substances are at chemical equilibrium and the forward and backward reaction rates of a particular isotope are identical. Kinetic isotope fractionation occurs usually during unidirectional processes, when the forward and backward reaction rates of a particular isotope are not identical. For example, liquid condensation in clouds is an equilibrium process because the liquid condensing in clouds is in equilibrium with vapor and evaporation is a kinetic process since the water vapor leaves permanently the residual reservoir (e.g., ocean). In addition, isotopically lighter molecules have higher vibrational energies and lower dissociation energies, which cause them to form weaker bonds that are more easily broken. During the evaporation process, light oxygen isotopes ($\delta^{16}O$) will preferentially evaporate from the surface of a liquid into the vapor phase, leaving the residual reservoir ^{18}O –rich. During condensation, the condensate becomes increasingly ^{18}O-rich, (because ^{18}O has a higher vapor pressure), while the water vapor becomes increasingly ^{18}O-depleted (Sharp, 2007).

Oxygen isotope values are expressed using "δ" (delta) notation. Variations in oxygen isotope ratios ($^{18}O/^{16}O$) are referenced against the international standard Vienna Standard Mean Ocean Water (VSMOW) for which a 0‰ value is attributed. The oxygen isotope values of other internationally certified standards are determined relative to VSMOW and the sample oxygen isotopic ratio is reported as a deviation from VSMOW. The delta notation is a useful method of expressing the relative differences in isotope ratios among samples and standards. The relative differences in isotope ratios are given by the equation:

$$\delta^{18}O‰ = [(({}^{18}O/{}^{16}O)_{sample} - ({}^{18}O/{}^{16}O))_{standard} / ({}^{18}O/{}^{16}O)_{standard}] \times 1000$$

where *sample* indicates the sample oxygen isotope abundance and *standard* indicates the standard oxygen isotope abundance (Sharp, 2007). The values of delta are reported in parts per thousand (per mil), indicated by the symbol "‰". A positive delta value indicates that the sample has more of the heavy oxygen isotope (^{18}O) than the reference standard. Negative delta values indicate that the sample has more of the light oxygen isotope (^{16}O) than the reference standard.

1.7 Oxygen Isotopes in the Hydrosphere

The concentration of ^{16}O and ^{18}O in proxies such as trees, water, ice and soil is a function of both the climate and the physical environment from which the proxy was extracted. The International Atomic Energy Agency's Global Network of Isotopes in Precipitation (IAEA-GNIP) has defined a set of environmental parameters that characterize observed isotope dispersal in space and time, which includes seasonality, amount of precipitation, altitude dependence, continentality, and local air temperature. The main parameters that affect oxygen isotope variation in the tropics are seasonality, temperature, and the amount of precipitation. It has been suggested that in tropical regions, isotopic temperature effects may be overridden by the amount effect due to wet season precipitation amount and warm temperatures coinciding (Vuille et al., 2003).

Meteoric Water

Meteoric water is the liquid or solid water that will fall or has already fallen from the sky, including rain, fog, hail, sleet, and snow (Sharp, 2007). Estimates of mean amounts and isotopic

compositions of precipitation around the world have led to a global oxygen isotopic composition of meteoric water of -8‰ (Sharp, 2007). The IAEA-GNIP has recorded worldwide variations in the $\delta^{18}O$ values of meteoric water since 1961 (Fig. 1.6). In the tropics, the amount of precipitation is inversely correlated with $\delta^{18}O_{meteoric}$ values for monthly (Gat, 1996) or individual rain events (Dansgaard, 1964; Managave and Ramesh, 2011). This variation in $\delta^{18}O_{meteoric}$ values is likely to leave its imprint on the oxygen isotope concentration of alpha-cellulose as no further isotope fractionation of the will occur once the roots of trees take-up soil water (State Key Laboratory of Hydrology-Water Resources and Hydraulic Engineering).

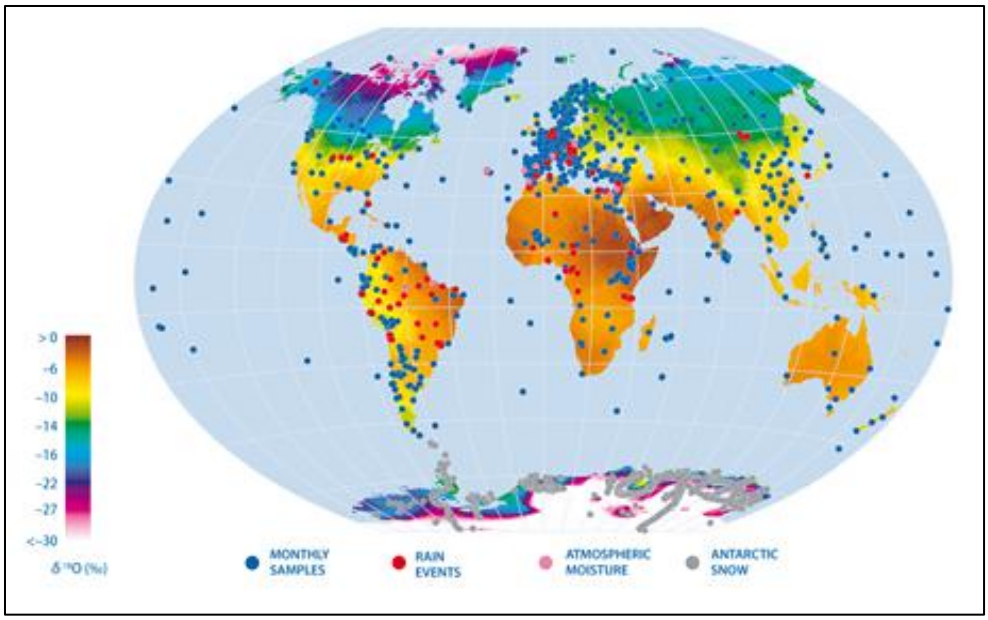

Figure1.6 Global distribution of oxygen-18 (per mil, ‰) in precipitation produced by interpolation of long-term annual means from about 700 GNIP stations. (IAEA-GNIP).

Early research on isotopes in tree rings determined that oxygen isotopes in alpha-cellulose may recorder the oxygen isotopic composition of meteoric water (Dansgaard, 1964; Libby et al., 1976;

Burke and Stuiver, 1981; McCarroll and Loader, 2004). Saurer et al. (2002) observed that differences in tree ring $\delta^{18}O$ values were related to variations in meteoric water $\delta^{18}O$ inputs, which also correlated with continental temperature variation. A positive relationship between $\delta^{18}O_{meteoric}$ values and temperature is the result of continuous isotopic depletion of cloud water during precipitation events (Saurer et al. 2002; Fig. 1.7).

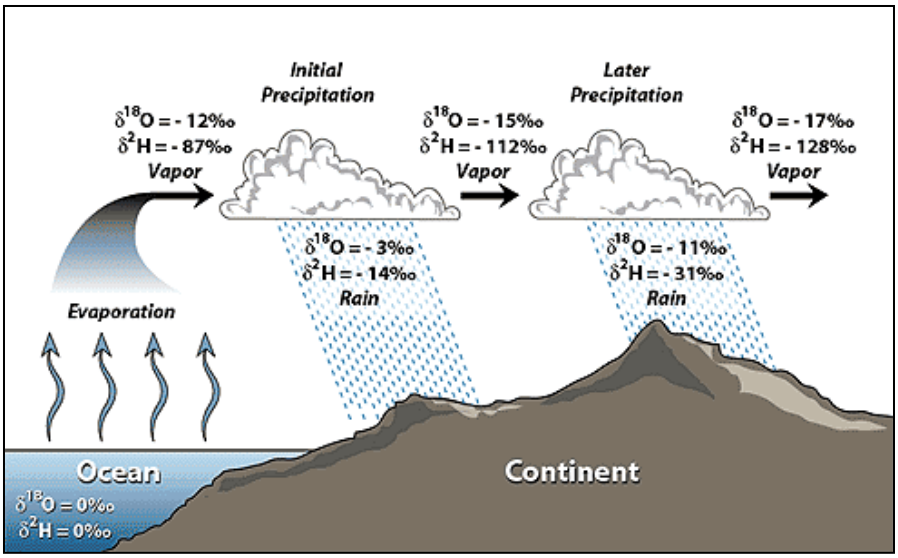

Figure 1.7 Isotopic Amount effect on $\delta^{18}O$ values in precipitation (based on Hoefs, 1997 and Coplen et al., 2000).

Condensation

As an air mass rises and cools, it moves away from its original vapor source. If the temperature of that air mass drops to the dew point, the air will become saturated and precipitation will eventually occur. When the first initial amounts of water vapor condense, the condensate will be $H_2{}^{18}O$-enriched and more positive that its original vapor source (Sharp, 20007). As further condensation occurs, water vapor preferentially looses the heavy $H_2{}^{18}O$ isotopologues, and the

ensuing water vapor and condensate become increasingly more and more $H_2{}^{18}O$-depleted because the heavier water molecules are continuously removed from the system (Dansgaard, 1964; Fig. 1.7). Condensation is an equilibrium process, meaning there is isotopic exchange between atmospheric vapor and liquid.

Evaporation

As mentioned previously, lighter water molecules ($H_2{}^{16}O$) have higher vapor pressures and translational velocities than the heavier water molecules ($H_2{}^{18}O$). This means that lighter water molecules preferentially escape from the surface of liquid water into the vapor phase. As a result of the evaporative enrichment in $H_2{}^{16}O$, evaporated water is relatively ^{18}O-depleted compared to residual water. Evaporation is a unidirectional process, meaning that continuous exchange between vapor and liquid does not occur (Sharp, 2007).

Temperature

The oxygen isotopic composition of precipitation is usually correlated with air temperatures, mainly in the sense that air temperature influences the amount of water vapor in a parcel of air. The dominant influence on the oxygen isotopic composition of precipitation from a given air parcel is the fraction of vapor remaining containing lighter isotopes in that air parcel (Sharp, 2007). Water vapor molecules containing heavier oxygen isotopes ($H_2{}^{18}O$) condense more readily than water molecules containing lighter oxygen isotopes ($H_2{}^{16}O$). Therefore rain events will progressively produce precipitation and clouds containing water vapor with ^{18}O-depleted water. Previous studies have shown significant correlations between the weighted mean oxygen isotopic

composition of precipitation and mean annual surface temperature at that particular location (Dangaard, 1964). For example, Saurer et al., (2002) found that $\delta^{18}O$ values in trees growing in Eurasia were strongly related to the $\delta^{18}O$ values of precipitation ($r = 0.99$, $p < 0.01$) and, accordingly, to annual temperature ($r = 0.90$).

In addition to precipitation becoming progressively ^{18}O-rich (^{18}O-depleted) with increasing (decreasing) temperature, temperature can also alter the $\delta^{18}O_{meteoric}$ values in soil water. Soil water utilized by trees can vary considerably in $\delta^{18}O$ values compared to the $\delta^{18}O$ values of precipitation due to the evaporative enrichment in ^{18}O of soil water (Burke and Stuiver, 1981; Roden and Ehleringer, 1999; McCarroll and Loader, 2004; Daux et al., 2011). The light $H_2{}^{16}O$ molecules will preferentially evaporate, leaving the soil water rich in $H_2{}^{18}O$ molecules. Therefore, the oxygen isotopic composition of soil water could become progressively ^{18}O-enriched with increasing temperature amount and frequency of the rain events, and type of soil. Therefore all these factors can have an effect on the oxygen isotopic composition of the soil water utilized by trees (Tang and Feng, 2001; McCarroll and Loader, 2004).

Continentality Effect

As air masses are move inland from the ocean, they become increasingly ^{18}O-depleted due to the progressive loss of moisture (Fig. 1.7). The difference in temperature between the ocean and continental location is a dominating factor. During cold months, the continentality effect is stronger because of steeper temperature gradients. During warm months, the continentality effect is reduced. Orographic lifting and subsequent cooling of the air also leads to ^{18}O-depleted vapor in air masses (International Atomic Energy Agency).

Latitude Effect

As temperatures typically decrease with latitude, the oxygen isotope values of precipitation decrease as well because of the increasing degree of "rain-out" (International Atomic Energy Agency). Therefore, as latitude increases, progressive condensation of the vapor leads to ^{18}O-depleted precipitation.

Altitude Effect

The oxygen isotopic composition of precipitation varies with altitude and becomes progressively ^{18}O-depleted and altitude increases. The altitude effect is temperature dependent because as an air mass rises and cools adiabatically (especially during orographic lifting), the amount of water vapor in that air mass decreases (International Atomic Energy Agency).

Amount Effect

Dansgaard (1964) observed a negative relationship between the amount of precipitation and $\delta^{18}O_{meteoric}$ values. The greater the amount of precipitation, the lighter $\delta^{18}O$ values of precipitation (Fig. 1.7). Saurer et al., (2012) found that the dominating influence on $\delta^{18}O_{\alpha c}$ in trees growing at three different locations in Switzerland was the oxygen isotopic composition of precipitation. Rinne et al., (2013) developed a 400-year May-August precipitation reconstruction using $\delta^{18}O_{\alpha c}$ values in trees growing in southern England. Their results demonstrated a highly significant correlation between Spring and Summer precipitation amount and $\delta^{18}O_{\alpha c}$ values ($r = -0.71$).

Seasonality Effect

In tropical regions, the seasonal variation in the oxygen isotopic composition of precipitation is dependent on the local temperature and the amount of monthly precipitation (Barbour et al., 2004; Poussart et al., 2004). Precipitation over Zimbabwe has ^{18}O-depleted values during the wet season and ^{18}O-enriched values during the dry season. Saurer et al. (2012) identified a seasonal effect on the $\delta^{18}O$ values of precipitation for three locations in Switzerland, with the most ^{18}O-depleted values in winter months and the most ^{18}O-enriched values in summer months. Interannual variability in average $\delta^{18}O$ of precipitation during the summer months was between one and four per mil and, in comparison, the seasonal variability in average $\delta^{18}O$ of precipitation was much larger.

Seasonal differences in precipitation also effect the in $\delta^{18}O$ values in soil water. Hsieh et al., (1998) in their analysis of $\delta^{18}O$ values of soil water in Hawaii found that low soil water content and heavier $\delta^{18}O$ values reflected the dry winter season. High soil water content and lighter $\delta^{18}O$ values were typical during the wet season.

1.7 El Niño Southern Oscillation/SST

Past studies have shown that in tropical regions La Niña events are associated with lighter $\delta^{18}O_{\alpha c}$ values and El Niño events are associated with $^{18}O_{\alpha c}$-enriched values (Evans and Schrag, 2004; Brienen et al., 2012). In the tropics, the isotopic effects of the ENSO events dominates the isotopic effects of the precipitation amount. Therefore, warmer than normal or cooler than normal ENSO events should be recorded in $\delta^{18}O$ values of alpha-cellulose. As mentioned previously, precipitation amount in southern Africa usually decreases during El Niño events, leading to ^{18}O-

enriched precipitation, and increases during La Niña events, leading to ^{18}O-depleted precipitation (Evans and Schrag, 2003). Because of the ENSO's effect on precipitation amount in tropical regions, it's possible that the variations in $\delta^{18}O$ values of alpha-cellulose can record the variations in the oxygen isotopic composition of precipitation due to ENSO events.

Evans and Schrag (2004) analyzed a range of tree genera from different tropical locations of the Neotripcs and identified an 8-9‰ anomaly in $\delta^{18}O_{\alpha c}$ values during the strong 1997-1998 ENSO warm phase in northwestern coastal Peru. In their study on $\delta^{18}O_{\alpha c}$ in *Fokienia hodginsii* (Po mu) growing in northern Laos, Xu et al., (2011) identified significant positive correlations between the $\delta^{18}O_{\alpha c}$ values and the average $\delta^{18}O$ values of precipitation during prior winter (December, January, February; $p < 0.05$) and premonsoon (March, April, May) Niño 3.4 sea surface temperatures (SSTs; $p < 0.05$). Brienen et al., (2012) found significant positive correlations between $\delta^{18}O_{\alpha c}$ in *Cedrela odorate* (tropical cedar) growing in the Amazon basin and SST ($p < 0.001 – 0.05$) in the central equatorial Pacific (Niño 3.4 region). They also found that the effect of ENSO on precipitation amount at the study site was relatively weak but the correlation between $\delta^{18}O_{\alpha c}$ values and ENSO was strong. Their results suggest the potential of using $\delta^{18}O_{\alpha c}$ as a proxy to illustrate historical influences of ENSO on precipitation variability in the tropics (Brienen at al., 2012).

1.9 Soil Hydrological Processes

Soil hydrological processes can also alter the oxygen isotopic composition of soil water utilized by trees. The oxygen isotopic composition of soil water is dependent upon the oxygen isotopic composition of meteoric water and groundwater (Managave and Ramesh, 2011). As a result of evaporative enrichment in the upper soil layers, a gradient exists where the upper layers of soil are $H_2{}^{18}O$-enriched compared to deeper soil layers (Fig. 1.8). The extent of the $\delta^{18}O$ soil-water

gradient depends on soil moisture content, soil composition and texture, and variations in precipitation $\delta^{18}O$ values (Managave and Ramesh, 2011). In their study on the effects of soil hydrological processes on the oxygen isotopic composition of soil water, Tang and Feng (2001) demonstrated that 1) soil water oxygen isotopic composition is much less variable than that of precipitation, suggesting a mixing of waters from different precipitation events; 2) soil water is ^{18}O-enriched due to infiltration of wet season precipitation and evaporation effects; 3) at increasing soil depths, the isotopic influence of wet season precipitation decreases, and only soil between 0 – 0.5 m in depth will record the isotopic signature of "new" precipitation; and 4) precipitation during the wet season gradually replaces dry season soil water, the amount of which is dependent upon the intensity and frequency of precipitation events during the growing season. These results are important because different levels of soil water may have varying oxygen isotope compositions, which will influence the $\delta^{18}O$ values of alpha-cellulose.

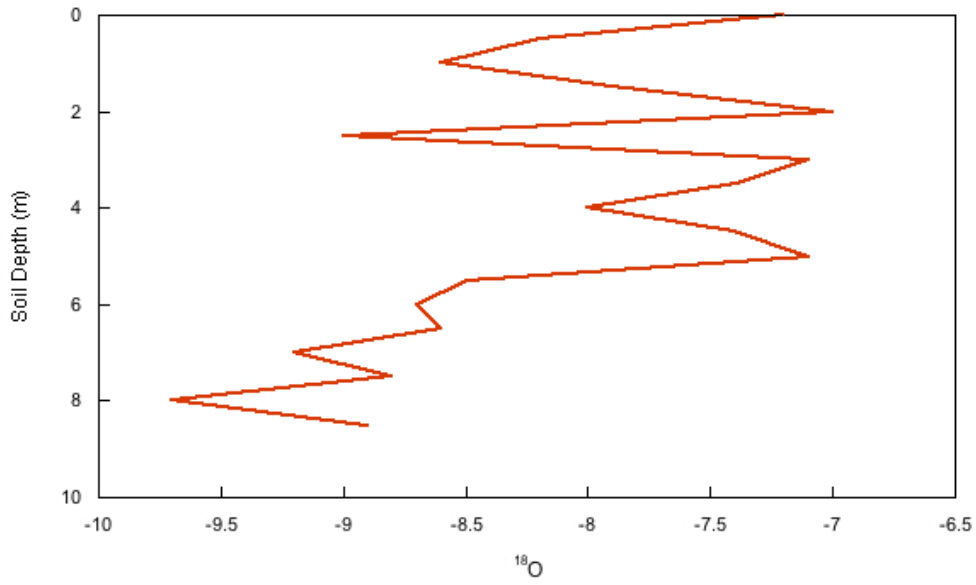

Figure 1.8 The relationship between soil depth and the oxygen isotopic composition of soil water and ground water (Nanjing Hydraulic Research Institute).

Hsieh et al., (1998) analyzed how precipitation recharge and mixing with antecedent soil water affects the oxygen isotopic composition of soil water. Their results showed that $\delta^{18}O$ values of water molecules in precipitation are always ^{18}O-depleted compared to soil water $\delta^{18}O$ values, with a differences of ~4-5‰. ^{18}O-depleted precipitation mixes with soil water that is ^{18}O-enriched due to evaporative effects, and the soil water then represents a mixture of these two sources (Hsieh et al., 1998).

CHAPTER 2

METHODOLOGY

2.1 Tree Ring Sampling and Extraction of Alpha-Cellulose

Two wedge-shaped partial cross sections (samples MZO30 and MZO35) collected from cut stumps and felled logs of *P. angolensis* were used in this study (Mushove et al., 1997 Fig. 2.1). The cross sections were chosen for isotopic analysis based upon a well-defined ring structure and length of record. Both samples were analyzed using the same standard dendrochronological techniques, including the skeleton plot method of cross-dating (Stokes and Smiley, 1996). Ring-width indices and age models from the exactly dated Mukwa tree rings were obtained from a previous study conducted by Therrell et al. (2006).

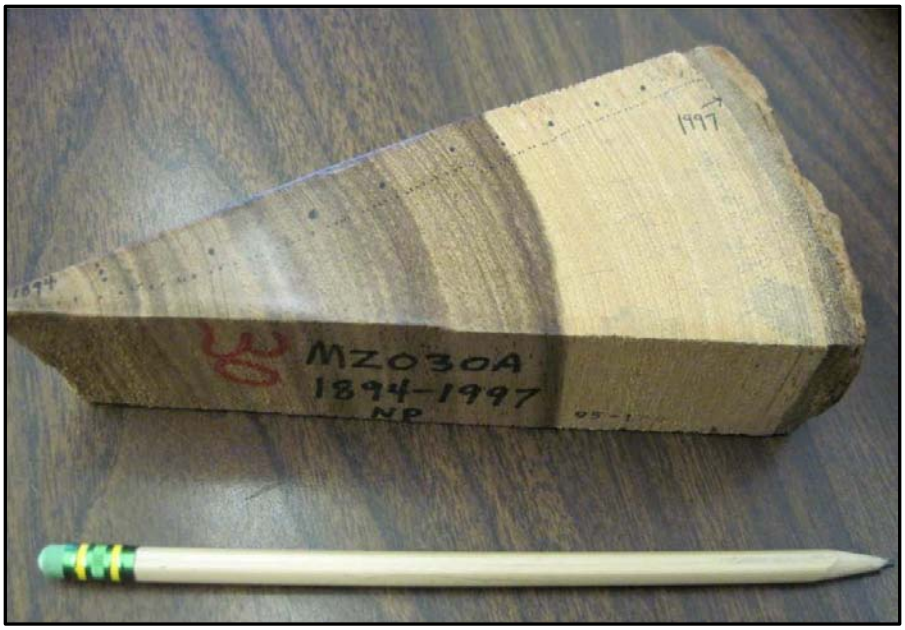

Figure 2.1 Partial cross-section of *Pterocarpus angolensis* (sample MZO30) from the Mzola forest.

In this study, I chose to extract alpha-cellulose from the whole-ring instead of separating each ring into early and late wood, for several reasons. First, it has been demonstrated in past studies that separating early wood from late wood is not required for isotopic analysis, because very strong and coherent isotopic correlations have been identified between both wood elements (Anderson et al., 1998; Kress et al., 2009b). Second, the isolation of a single chemical element component, in this instance alpha-cellulose, reduces problems associated with variability in the lignin:cellulose ratio that can happen inter-annually, among individual trees or within a sequence through time (McCarroll and Loader, 2004). Third, greater homogeneity of the sample is achieved during the alpha-cellulose purification process (McCarroll and Loader, 2004).

Previous research on isotopic analysis of tree-rings (e.g., Libby and Pandolfi, 1974; Deniro and Epstein, 1979; Grootes et al., 1989; Sternberg, 1989) identified the importance of using alphacellulose in isotopic analysis as opposed to other wood constituents such as lignin or resins from whole wood. The oxygen components of lignin and resins are capable of isotopic exchange with atoms in water, while the oxygen in alpha-cellulose in non-exchangeable (McCarroll and Loader, 2004; Gaudinski et al., 2005; Horan, 2011). The use of whole wood in isotopic analysis produces a more ambiguous signal compared to alpha-cellulose alone (Loader et al., 1997). Additionally, Battipaglia et al., (2008) demonstrated that the extraction of alpha-cellulose from other wood components is necessary to ensure reliable reconstructions of past climatic conditions for deciduous trees. Their findings determined that alpha-cellulose had consistently stronger and less variable temporal correlations with climate parameters than whole wood.

Alpha-cellulose was extracted from the wood samples using the modified Brendel procedure (Brendel et al., 2000), which allows for rapid sample processing without the use of carcinogenic materials. The extraction methods separated the alpha-cellulose from lignins, resins, and cellulose

chains that may have different biochemical synthesis factors that influence $\delta^{18}O$ fractionation (Evans and Schrag, 2004; Horan, 2011). Finely sliced whole wood samples were extracted from each ring for the years 1955-1984 (Fig. 2.2). The samples, weighing between 400-1500 *μg*, were placed into 1.5 ml polypropylene microcentrifuge tubes and mixed with 120 μl 80% acetic acid and 12 μl 69% nitric acid. The tubes were capped, the lids taped, and placed in a Benchmark Scientific BSW1500 aluminum dry bath heating block at 119°C-124°C for 30 minutes. The sample tubes were removed from the heating block and allowed to cool to room temperature. 400 μl of 100% ethanol was added to remove extraction breakdown products (Brendel, 2000). The tubes were then recapped and centrifuged at 4500 rpm for five minutes in a 12-cell centrifuge. The supernatant was pipetted out of the sample tubes and 300 μl of distilled deionized water was added to each tube to remove traces of nitric acid. The samples were inverted, shaken, and centrifuged at 4500 rpm for five minutes. The samples were washed again by removing the supernatant and adding 150 μl of 100% ethanol to each tube. The samples were then centrifuged at 4500 rpm for five minutes. The supernatant was pipetted out and the samples rinsed in 150 μl of acetone to remove any remaining organic material and for sample dehydration. The supernatant was pipetted out and the samples were dried in an oven at 45°C for 30 minutes and then placed in a vacuum evaporator and covered with aluminum foil for overnight storage. The final samples appear white, cottony, and odorless. Each extraction process yielded 12 samples.

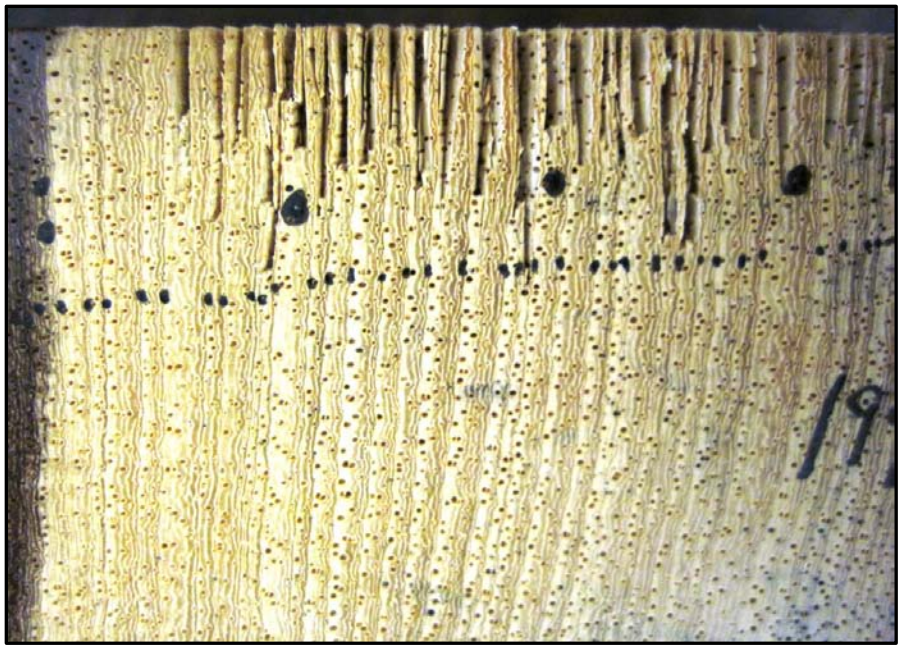

Figure 2.2 Finely sliced whole-wood samples, weighing between 400-1500 µg, were extracted for each year.

2.2 Stable Isotope Analysis

200-300 µg of dried alpha-cellulose extracted from each ring was placed into 3.5 x 5 mm Costech silver capsules and compressed gently into a tiny ball to remove any extraneous atmosphere (Horan, 2011). The samples were then loaded into a 50-cell Costech zero blank autosampler and the pyrolysis of samples to CO was performed in a ThermoFinnigan Thermal Conversion/Elemental Analyzer (TC/EA) at 1420°C. The $\delta^{18}O$ of the CO product was determined in continuous flow mode on a ThermoFinnigan Delta V Plus isotope ratio mass spectrometer coupled to the TC/EA via a ConFlo IV open split interface. The raw $\delta^{18}O$ values of cellulose samples were corrected based on pre- and post-sample $\delta^{18}O$ values of internationally certified standards for which the oxygen isotope composition is well known. The analytical precision was

±0.3 ‰ and was calculated taking into account the $\delta^{18}O$ values of a laboratory standard, aliquots of each were inserted within and processed together with the cellulose samples. Analytical precision is represented by the standard deviation of the data and is determined by analyzing standards repeatedly and comparing the standards performance to current performance (Fitzsimmons et al., 2000; U.S Dept. of Energy). Data values are reported on the Vienna Standard Mean Ocean Water (VSMOW) scale and in the standard delta notation.

2.3 Data

2.3.1 Alpha–Cellulose $\delta^{18}O$

Correlation analysis between $\delta^{18}O_{\alpha c}$ values from both cross-sections revealed that the annual $\delta^{18}O_{\alpha c}$ values of each cross-section were very similar ($r = 0.61$, $p < 0.001$), allowing averaging of the $\delta^{18}O_{\alpha c}$ values to create a single "chronology" for the years 1955-1984. To determine the potential usefulness of $\delta^{18}O_{\alpha c}$ as a climate proxy, the average oxygen isotope chronology was compared to ring-width, mean temperature, the oxygen isotopic composition of meteoric water, and total precipitation on monthly, seasonal, and annual time scales. The data were subjected to statistical evaluation and the data points were plotted based on Pearson's correlation coefficient *(r)*, with significance determined using Student's *t*-test to assess the relationship between meteorological parameters and $\delta^{18}O$ values in alpha-cellulose. In all instances, unless otherwise noted, the significance level is 0.05.

2.3.2 Ring-Width Data

To quantify whether $\delta^{18}O_{\alpha c}$ analysis improves statistical relationships to climatic parameters as opposed to ring-width analysis, the CRU 2.5° x 3.75° monthly gridded precipitation data were correlated against the ring-width measurements. The ring-width measurements of both *P. angolensis* samples used in this study were obtained from the NCDCs International Tree Ring Database (Mushove et al., 1997). Only ring width data for the period 1955-1984 were used (Tables 2.1 and 2.2). The ring- width series were compared to monthly precipitation totals as well as seasonalized (November-February) precipitation totals.

2.3.3 Climate Data

To investigate the influence of temperature on $\delta^{18}O_{\alpha c}$ values, I performed correlation analysis between monthly mean temperature data from the nearest meteorological station (Hwange, Zimbabwe; -18.633°, 27°, 1077 m asl, ~161 km from the study site) and the $\delta^{18}O_{\alpha c}$ chronology (Fig. 1.1). The data were obtained from the National Climatic Data Center (NCDC; National Oceanic and Atmospheric Administration), which included the period from 1962 to 1981.

To investigate the capacity of $\delta^{18}O_{\alpha c}$ values in tree rings to record a precipitation signature, the $\delta^{18}O_{\alpha c}$ chronology from 1955-1984 was compared to monthly instrumental precipitation data. The Climate Research Unit (CRU) 2.5° x 3.75° gridded resolution precipitation dataset (grid point -17.5° x 26.5°; constructed and supplied by CRU (University of East Anglia; Fig. 1.1) were utilized. Months with a significant relationship to $\delta^{18}O_{\alpha c}$ were combined and further analyzed to determine the seasonal response recorded in $\delta^{18}O_{\alpha c}$.

Monthly $\delta^{18}O_{meteoric}$ data for this region were obtained from the Global Network of Isotopes in Precipitation (International Atomic Energy Agency, IAEA) station in Harare, Zimbabwe (-17.83°,

31.02°, 1471 m asl, ~ 586 km from the study site; Fig. 1.1), and compared to the $\delta^{18}O_{\alpha c}$ chronology and monthly precipitation amount. The $\delta^{18}O_{meteoric}$ values were compared to the $\delta^{18}O_{\alpha c}$ chronology to identify the efficiency of *P. angolensis* in capturing a record of the $\delta^{18}O$ signature in meteoric water. To test for the amount effect, the $\delta^{18}O_{meteoric}$ values were compared to monthly precipitation totals. To further test whether $\delta^{18}O$ in α-cellulose captures a record of annual oxygen isotope values in meteoric water, the $\delta^{18}O_{\alpha c}$ chronology was compared to annual $\delta^{18}O_{meteoric}$ data, which were also obtained from the IAEA station in Harare (Fig. 1.1).

2.3.4 SST Data

To identify any relevant large-scale forcings on the $\delta^{18}O$ in the alpha-cellulose of *P. angolensis*, NOAAs Monthly/Seasonal SST Climate Composites was utilized to compare SST anomalies and variability in the $\delta^{18}O_{\alpha c}$ values. The five most $^{18}O_{\alpha c}$-depleted values and the five most $^{18}O_{\alpha c}$-enriched values from the 30-year chronology were chosen for analysis (Table 2.3). The climate variable used in analysis was the NOAA Extended SST, the level was 'Surface', and the months analyzed were November to February.

Table 2.3 The five most $^{18}O_{\alpha c}$-depleted and five most $^{18}O_{\alpha c}$-enriched values and associated years during the 30-year chronology

Five Most $18O_{\alpha c}$-Enriched Values		Five Most $^{18}O_{\alpha c}$-Depleted Values	
Year		Year	
1962	33.23	1955	25.73
1965	34.57	1956	25.87
1967	32.24	1958	24.5
1973	34.11	1959	24.75
1977	31.48	1974	26.33

CHAPTER 3

RESULTS

3.1 Isotope Chronology

The individual $\delta^{18}O_{\alpha c}$ chronologies did not exhibit significant differences from one another ($r = 0.61$, $p < 0.0002$), confirming a high synchronicity between both $\delta^{18}O_{\alpha c}$ isotope chronologies, and therefore the mean $\delta^{18}O_{\alpha c}$ values of both samples were used for analysis (Table 3.1; Fig. 3.1). The mean $\delta^{18}O_{\alpha c}$ values varied from 24.50‰ (1958) to 34.57‰ (1965), with a mean of 29.32‰ and standard deviation of 2.56‰ (Table 3.2). Annual climate signals retained in the $\delta^{18}O$ of alpha-cellulose are expected to vary because of their sensitivity to environmental conditions, such as fluctuations in precipitation and temperature, at the time of their formation (An et al., 2012). The data in Fig. 3.1 show a slight positive trend in $\delta^{18}O_{\alpha c}$ values of 0.06‰ between 1955-1984.

3.2 Ring-Width Chronology

Although the two individual ring-width series did not exhibit as strong of a correlation with one another as did the individual $\delta^{18}O_{\alpha c}$ series ($r = 0.41$, $p = 0.02$, $n = 30$), an average of the series was used for analysis. The ring-width values of the averaged chronology varied from 0.48 mm (1984) to 2.67 mm (1980), with a mean of 1.45 mm and standard deviation of 0.53 mm. Year to year variability was as high as 7.78 mm. The average ring-width chronology was weakly negatively correlated with the $\delta^{18}O_{\alpha c}$ chronology ($r = -0.04$; Fig. 3.2).

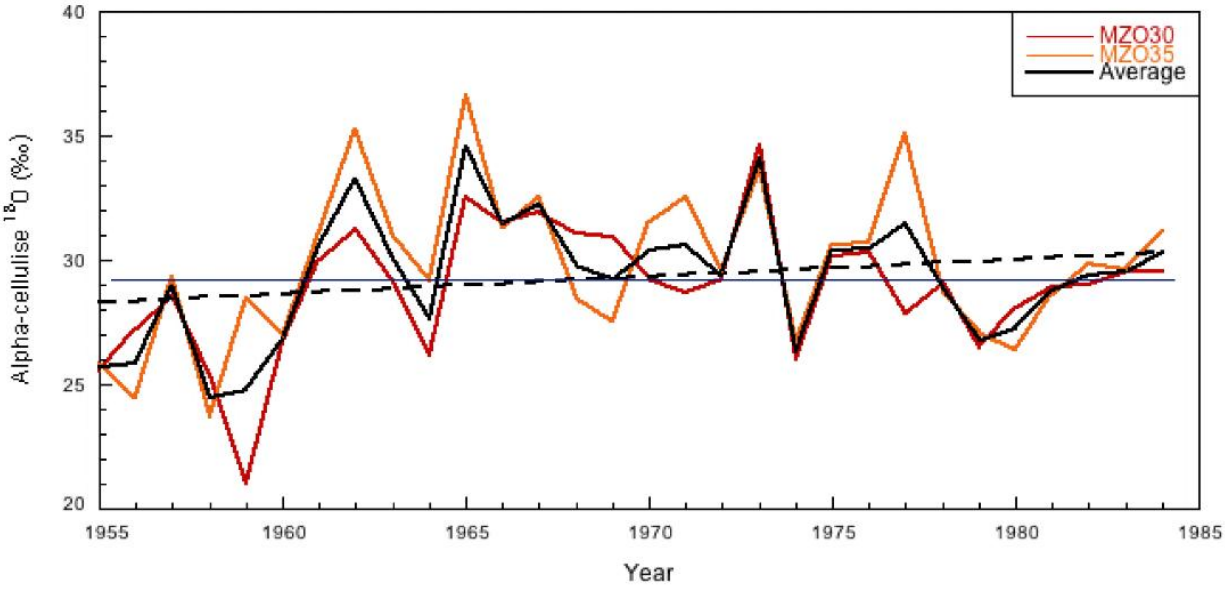

Figure 3.1 Time series of $\delta^{18}O_{\alpha c}$ values from two partial cross-sections (MZO30 and MZO35) and the average $\delta^{18}O_{\alpha c}$ values of both cross-sections (black bold line). Black dashed line represents the increasing trend in $\delta^{18}O_{\alpha c}$ values during the 30-year study period. The blue line represents the average $\delta^{18}O_{\alpha c}$ value of both sample series.

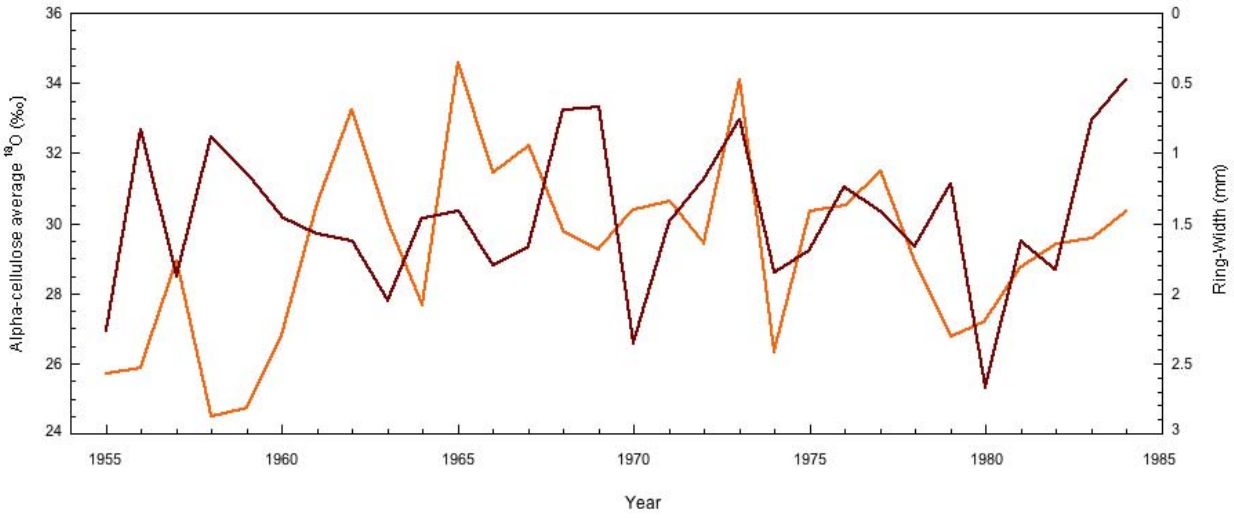

Figure 3.2 Variations in the $\delta^{18}O_{\alpha c}$ chronology (orange line) and ring-width chronology (brown line) during the 30-year study period

3.3 Correlations between Ring-Width and Precipitation

The ring-width chronology displayed significant variation throughout the 30-year study period. Correlation analysis of monthly precipitation totals and the ring-width chronology revealed that the strongest correlation was found near the beginning of the wet season (prior calendar year December; r = 0.45, p = 0.01, n = 30; Fig. 3.3). The ring-width chronology was significantly correlated with prior year November to December total precipitation (r = 0.52, p = 0.003).

The ring-width values were not significantly correlated with total wet season (November to April) precipitation amount (r = 0.20, p = 0.29, n = 30; Fig. 3.4), November to February precipitation (r = 0.3, p = 0.11, n = 30), nor the ten wettest or ten driest wet seasons (r = -0.03 and r = -0.06, respectively). I did not identify a significant correlation between ring-width and annual (November to October) precipitation (r = 0.2).

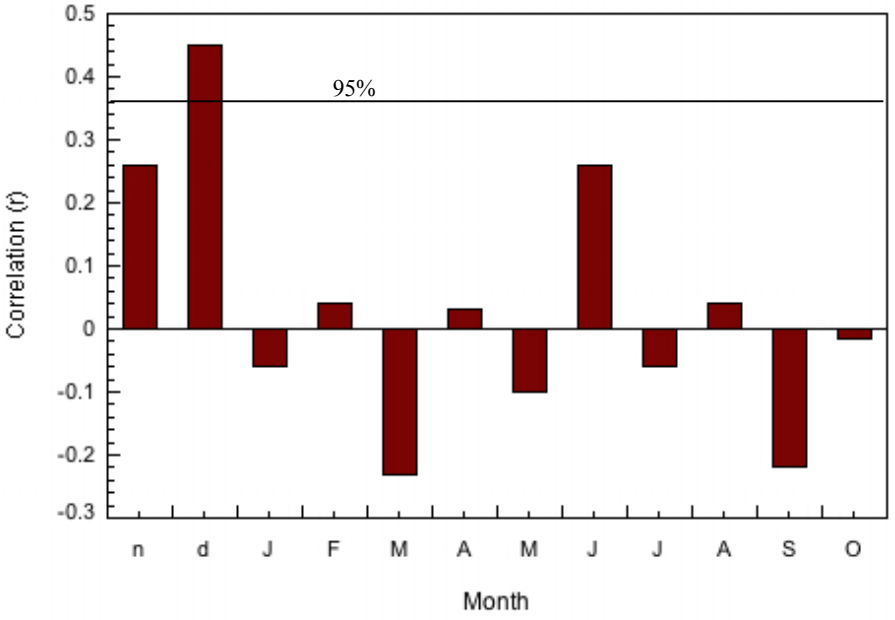

Figure 3.3 Correlation (r) between monthly precipitation amount and ring-width for the years during the 30-year analysis period. Solid black line represents the 95% confidence limit.

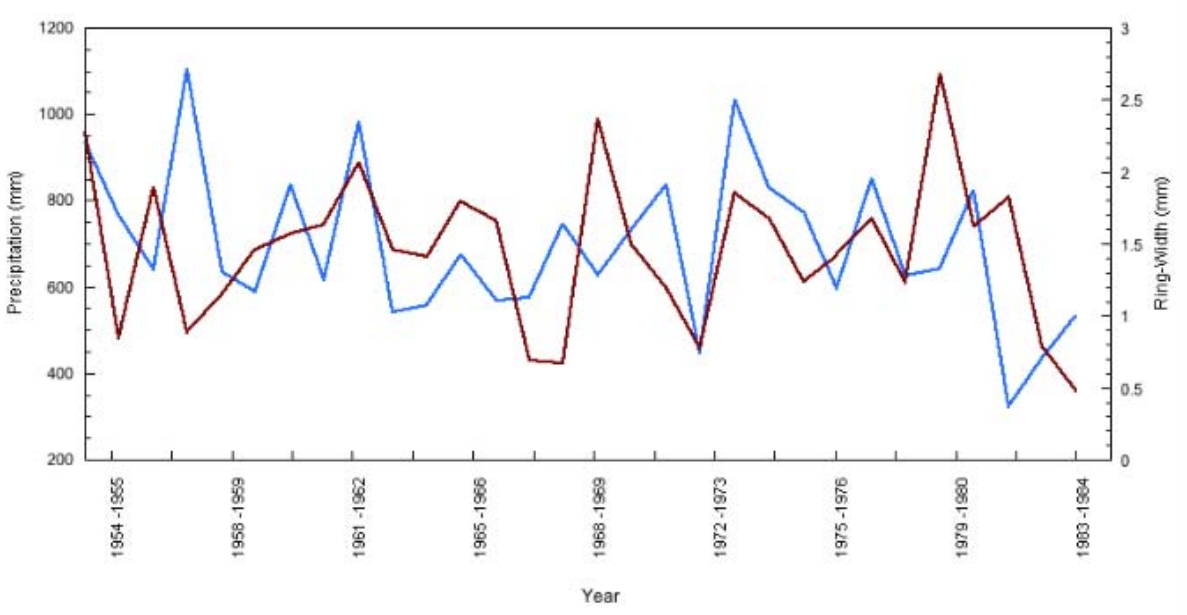

Figure 3.4 Variations in the seasonal (November to April) precipitation amount (blue line) and ring-width chronology (brown line) during the 30-year study period.

3.4 Correlations with Temperature

The $\delta^{18}O_{ac}$ chronology was significantly correlated with monthly mean temperature (but not tmax or tmin) and the correlation coefficients increased when the temperature data were seasonalized to correspond to the summer wet season (November to April). The strongest correlations between the $\delta^{18}O_{ac}$ chronology and mean monthly temperature were identified near the beginning (previous calendar year) December ($r = 0.49$, $p = 0.03$, $n = 18$) and end (current year June; ($r = 0.52$, $p = 0.03$; $n = 17$; Fig. 3.5) of the growing season. The correlation between wet season temperature and the $\delta^{18}O_{ac}$ chronology is statistically significant ($r = 0.56$, $p = 0.01$, $n = 18$), and suggests that mean wet-season temperature explains 31% of the variance in $\delta^{18}O_{ac}$ values (Fig. 3.6). The strongest correlation between wet season temperature and $\delta^{18}O_{ac}$ values were for mean temperatures greater than ~ 23.0°C. There was not a significant correlation between the $\delta^{18}O_{ac}$ chronology and the dry season mean temperature (May-October).

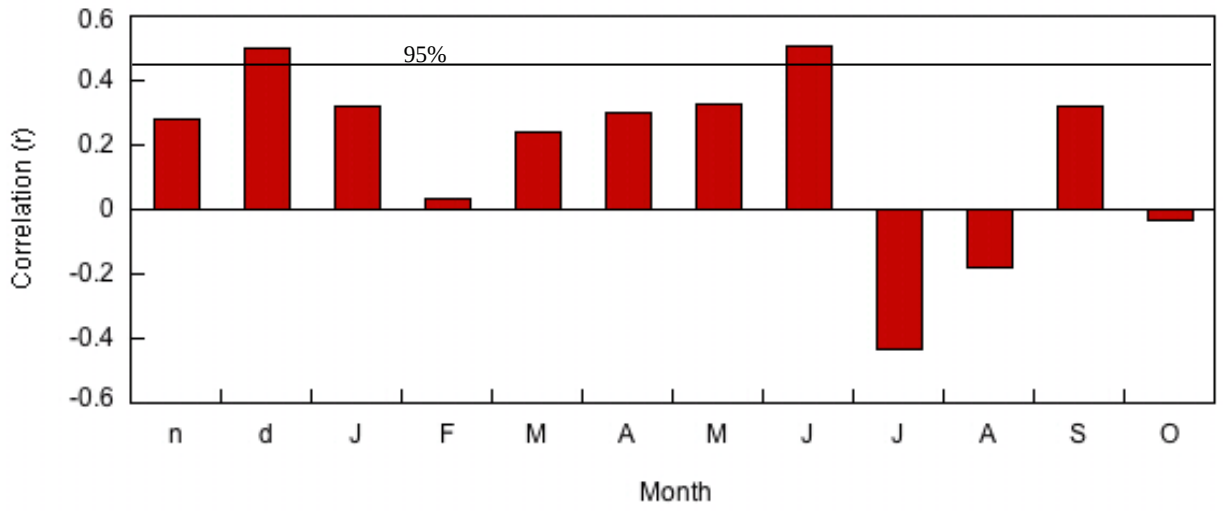

Figure 3.5 Correlation (r) between the $\delta^{18}O_{ac}$ chronology and mean monthly temperature (1963-1981). Solid black like represents the 95% confidence limit.

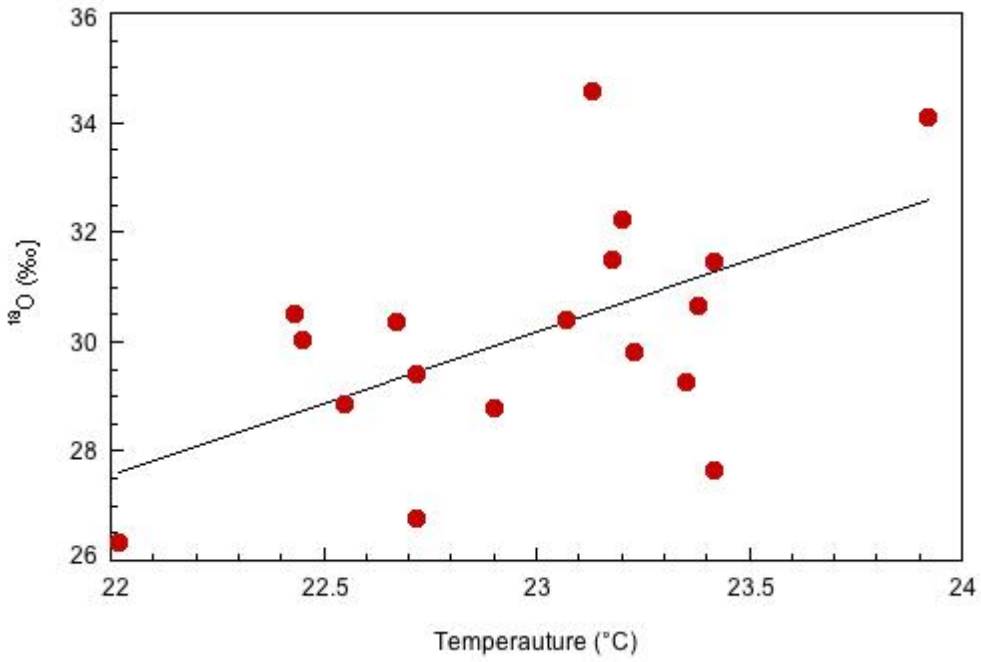

Figure 3.6: The relationship between wet season (November to April) mean temperature and the $\delta^{18}O_{\alpha c}$ chronology, 1963 – 1981 (r = 0.56, p = 0.01).

3.5 Correlations Between $\delta^{18}O_{\alpha c}$ and Precipitation

The $\delta^{18}O_{\alpha c}$ chronology also displays a highly significant negative relationship with February precipitation totals (r = -0.50, p = 0.005, n = 30; Fig. 3.7, Fig. 3.8). No other individual months were significantly correlated. The $\delta^{18}O_{\alpha c}$ chronology also displays a statistically significant inverse relationship with overall wet season precipitation amount (r = -0.45, p = 0.01, n = 30). Unusually rainy wet seasons (November to April) during our 30-year analysis period, where precipitation amount was well-above average, strongly correspond to $^{18}O_{\alpha c}$-enriched values, while noticeably dry summer seasons correspond to $^{18}O_{\alpha c}$-depleted values (Fig. 3.9). The ten wettest seasons between the years 1955-1984 were plotted versus the corresponding $\delta^{18}O_{\alpha c}$ values, identifying a highly significant inverse correlation (r = -0.80, P = 0.007; Fig. 3.10). I did not identify significant

correlations between the $\delta^{18}O_{\alpha c}$ chronology and dry season (May - October) precipitation totals (r = -0.12) nor the ten driest wet seasons (r = 0.003).

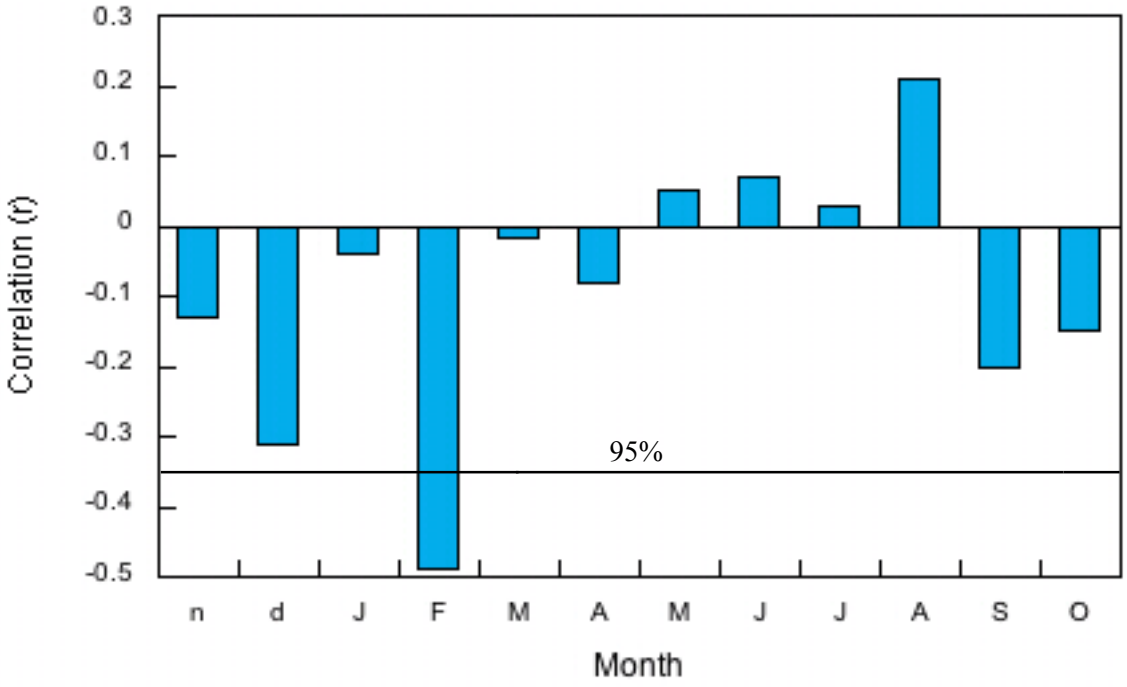

Figure 3.7 Correlation (r) between the $\delta^{18}O_{\alpha c}$ chronology and mean monthly precipitation during the 30-year study period. Solid black like represents the 95% confidence limit.

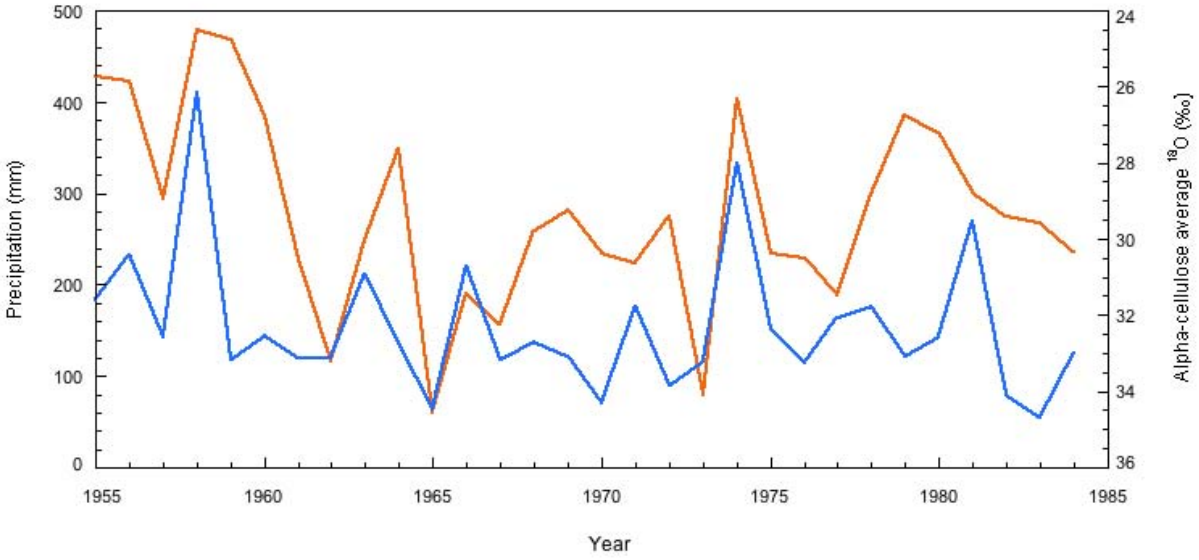

Figure 3.8 Variations in February precipitation amount (blue line) and the $\delta^{18}O_{\alpha c}$ chronology (orange line) over the 30-year study period. Correlation: r = -0.50, p = 0.005.

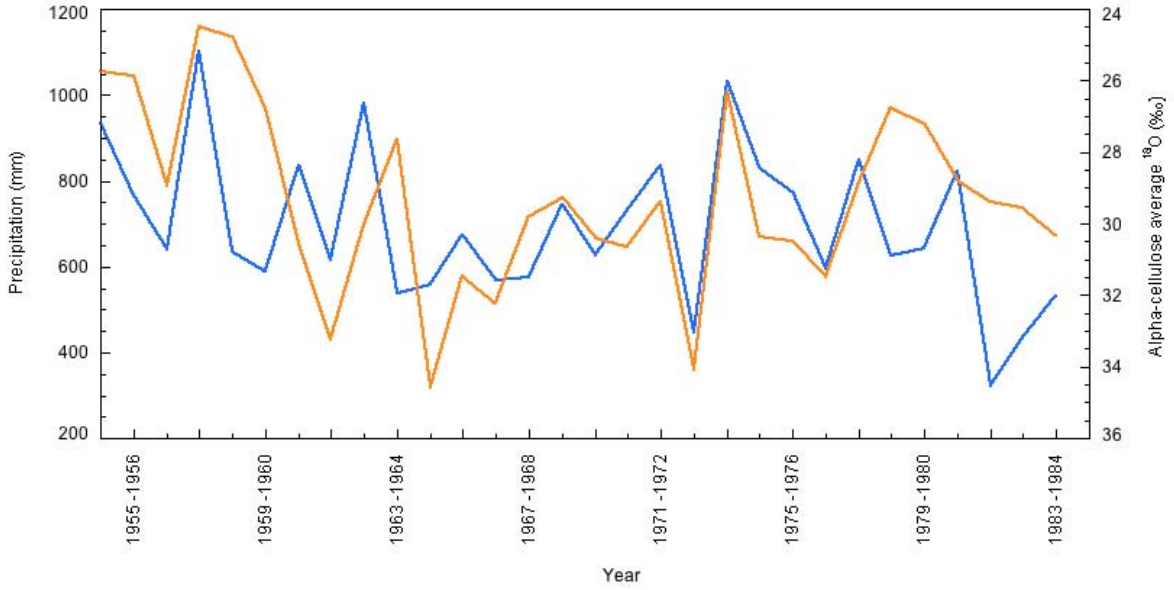

Figure 3.9 Variations in wet season (November to April) precipitation totals (blue line) and $\delta^{18}O_{\alpha c}$ chronology (orange line) over the 30-year study period.

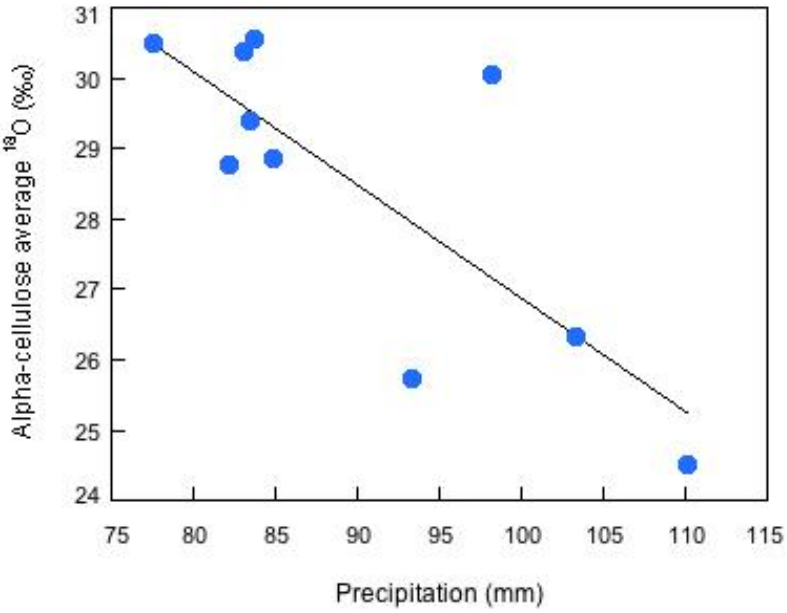

Figure 3.10 Relationship between the $\delta^{18}O_{\alpha c}$ chronology and the ten wettest summer seasons (November – April) during the 30-year study period. Correlation: r = -0.80, P = 0.007.

Well-above average annual (November to October) precipitation totals were found in the years 1955, 1958, 1963, and 1974 and well-above average wet season (November to April) precipitation totals were found in the years 1954-1955, 1957-1958, 1973-1974, 1977-1978, all of which correspond to $^{18}O_{\alpha c}$-depleted values. Both the highest seasonal and annual precipitation totals for the period under study occurred during 1957-1958 and correspond to the most $^{18}O_{\alpha c}$-depleted value during our 30-year analysis period (-24.05‰).

3.6 Correlations with Meteoric Water $\delta^{18}O$

Correlation between monthly $\delta^{18}O_{meteoric}$ values and the $\delta^{18}O_{\alpha c}$ chronology revealed that the strongest correlation is with previous December, (r = 0.68, p = 0.003, n = 17; Fig. 3.11), which is the month containing the highest total rainfall amounts for the period under study. Significant

correlations were also identified between seasonal mean $\delta^{18}O_{meteoric}$ values from November through January and December through February and the $\delta^{18}O_{\alpha c}$ chronology (r = 0.60, p = 0.02, n = 15) as well as annual (January through December) $\delta^{18}O_{meteoric}$ values (r = 0.50, p = 0.04, n = 17).

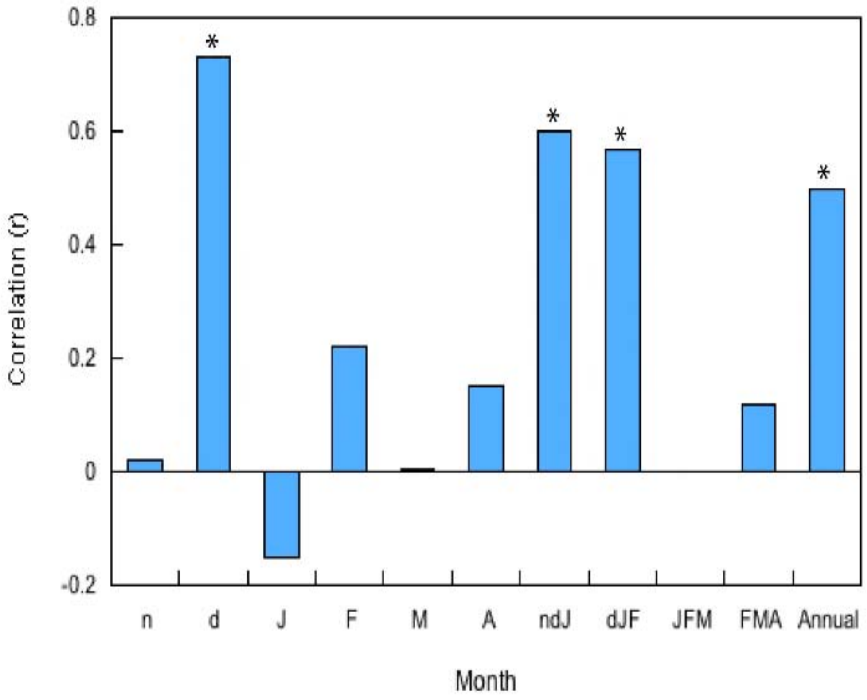

Figure 3.11 Correlation (r) between the $\delta^{18}O_{meteoric}$ values and $\delta^{18}O_{\alpha c}$ chronology for the years 1960-1968, 1971-1982. Annual: 1961-1978. Asterisk represent significance levels of ≤ 0.05.

To identify an isotopic amount effect, a correlation analyses was performed on the $\delta^{18}O_{meteoric}$ values and monthly precipitation totals (Fig. 3.12). The $\delta^{18}O_{meteoric}$ values demonstrate the amount effect where the average $\delta^{18}O_{meteroic}$ values were negatively correlated with precipitation amount. The strongest monthly correlations were identified between January $\delta^{18}O_{meteoric}$ values and January precipitation amount (r = -0.56, p = 0.01, n = 18) and April $\delta^{18}O_{meteoric}$ values and April

precipitation amount (r = -0.50, p = 0.03, n = 18). I identified a highly significant inverse relationship during November through January precipitation amount and annual $\delta^{18}O_{meteoric}$ values (r = -0.70, p = 0.004, n = 15) and annual (January to December) precipitation amount and annual $\delta^{18}O_{meteoric}$ val

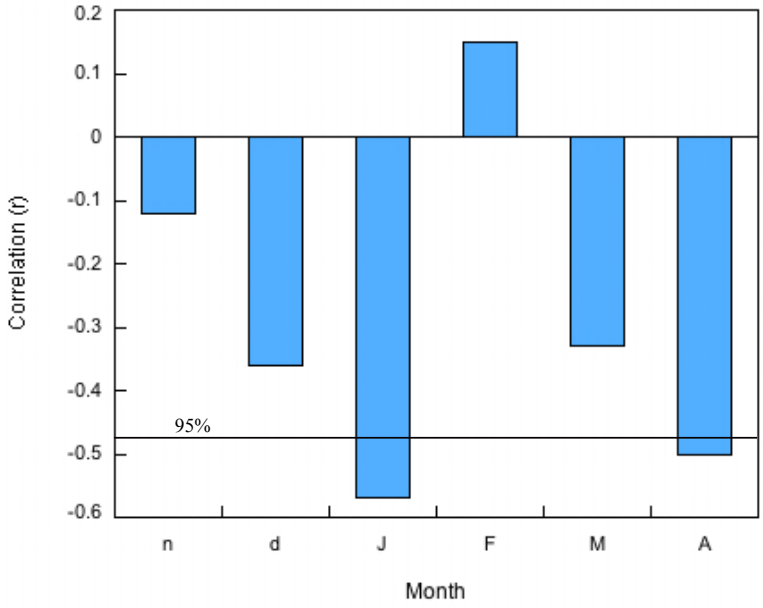

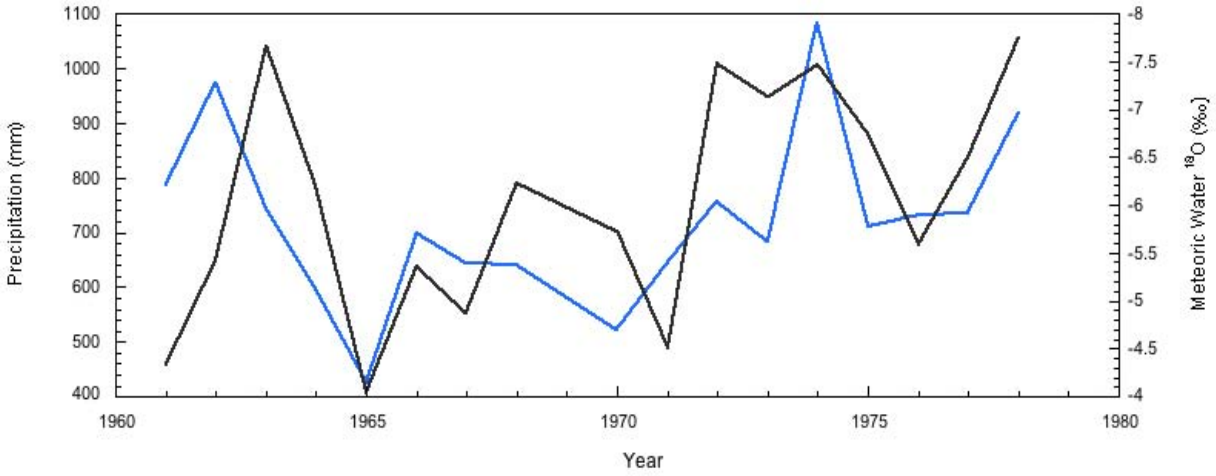

Figure 3.13 Variations in annual precipitation amount (blue line) and annual meteoric water $\delta^{18}O$ values (black line) for the years 1961-1978.

3.7 Relationship between SST and $\delta^{18}O_{ac}$ Values

Anomalous SSTs are associated with $^{18}O_{ac}$-enriched and $^{18}O_{ac}$-depleted values. Analysis suggests a positive relationship between SSTs in the equatorial Atlantic, Indian, South Pacific Oceans and $\delta^{18}O_{ac}$ values. Negative SST anomalies are associated with $^{18}O_{ac}$-depleted values (Fig. 3.14) and, conversely, positive SST anomalies are associated with $^{18}O_{ac}$-enriched values (Fig. 3.15). SST temperature anomalies in the Atlantic, Indian, South Pacific Oceans do not appear to be strongly related to precipitation amount in southern Africa during the years of the most $^{18}O_{ac}$-enriched and $^{18}O_{ac}$-depleted values.

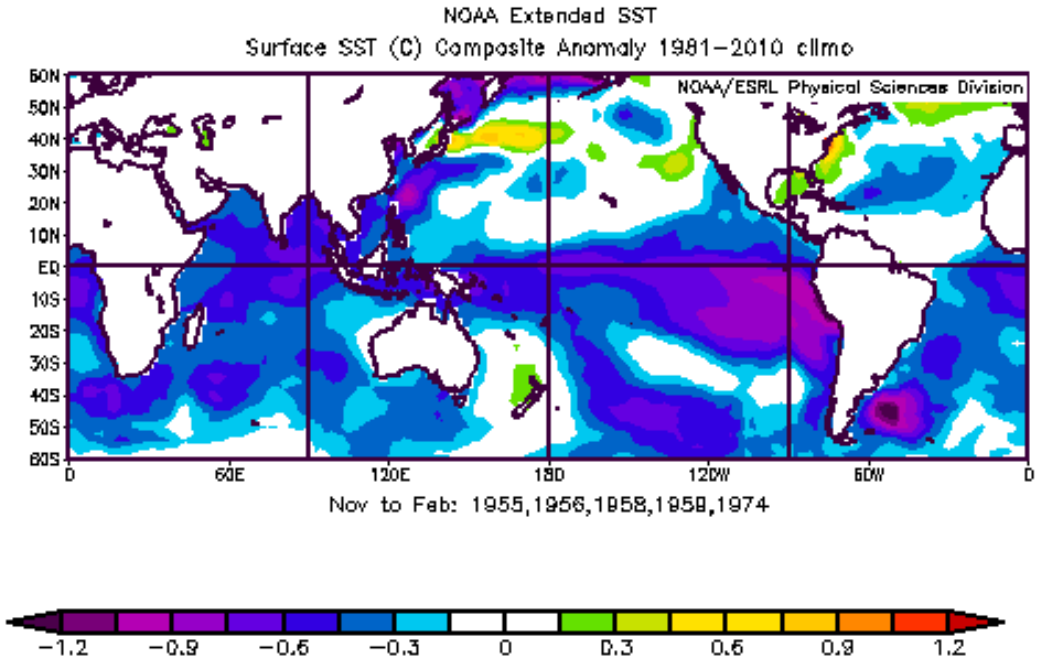

Figure 3.14 Composite seasonal SST anomalies during the wet season (November to February) of the five years with the most $^{18}O_{ac}$-depleted values of the 30-year chronology. The most $^{18}O_{ac}$-depleted values are (in ‰): 25.73 (1955); 25.87 (1956); 24.5 (1958); 24.75 (1959); 26.33 (1974). Image provided by the NOAA/ESRL Physical Sciences Division, Boulder Colorado from their Web site at http://www.esrl.noaa.gov/psd/.

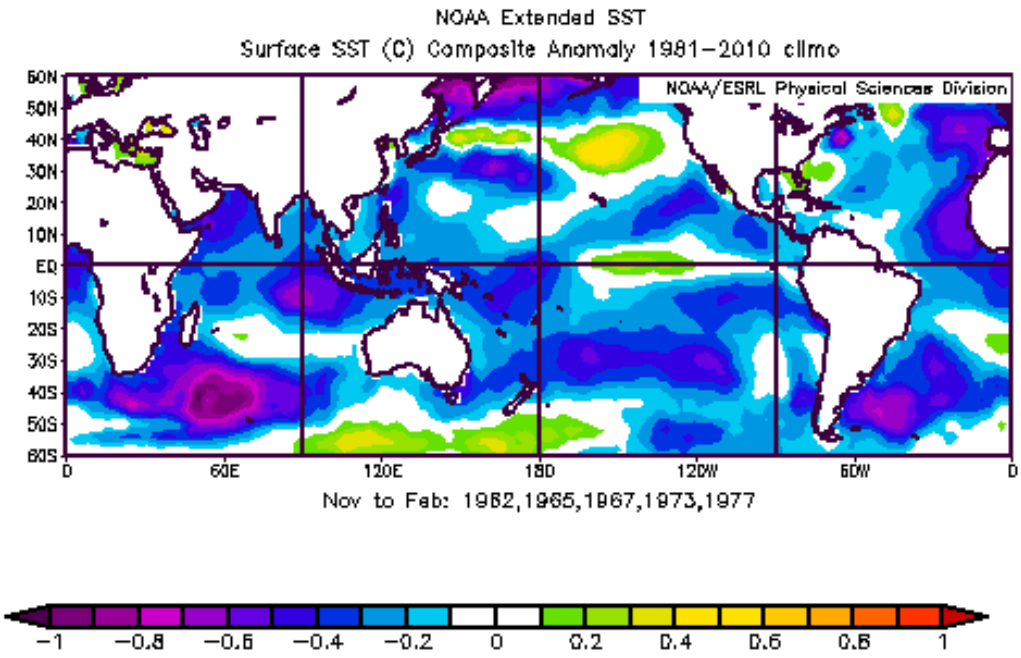

Figure 3.15 Composite seasonal SST anomalies during the wet season (November to February) of the five years with the most $^{18}O_{ac}$-enriched values of the 30-year chronology. The most $^{18}O_{ac}$-enriched values are (in ‰): 32.24 (1962); 34.57 (1965); 32.24 (1967; 34.11 (1973); 31.48 (1977). Image provided by the NOAA/ESRL Physical Sciences Division, Boulder Colorado from their Web site at http://www.esrl.noaa.gov/psd/.

CHAPTER 4

DISCUSSION

4.1 $\delta^{18}O_{\alpha c}$ Chronology

The individual $\delta^{18}O_{\alpha c}$ series did not exhibit significant differences from one another and the corresponding amplitude of annual $\delta^{18}O_{\alpha c}$ values between both samples suggests that *P. angolensis* are recording seasonal variations in $\delta^{18}O$ values during the 30-year record. The maximum interannual variation in $\delta^{18}O_{\alpha c}$ values is 7‰, which is comparable with the results of past studies (Robertson et al., 2001; Roden et al., 2005; Liu et al., 2008). My results support the notion that $\delta^{18}O_{\alpha c}$ values are sensitive to interannual variation in climatic variables such as mean wet-season temperature and rainfall totals. The main controls on the fractionation of oxygen isotopes depend on the conditions under which trees have grown and past studies have related interannual variations in $\delta^{18}O_{\alpha c}$ values to variations in precipitation amount and temperature (McCarroll and Loader, 2004; Daux et al., 2011; Brienen et al., 2012). The significant correlation between the two *P. angolensis* $\delta^{18}O_{\alpha c}$ series suggests that $\delta^{18}O_{\alpha c}$ *is* controlled by distinct common external forcings. This fact coupled with the long life span and annual ring structure of *P. angolensis* suggests that this species should be a good choice for tropical isotope dendroclimatology.

Past research has suggested that differences in oxygen isotope composition from individual trees within the same species growing at the same site can be as large as those between species (McCarroll and Loader, 2004). While both the $\delta^{18}O_{\alpha c}$ series are strongly correlated over the 30-year time period, there were some years when the $\delta^{18}O_{\alpha c}$ values were not as similar. In 15 of the 30-years analyzed, the $\delta^{18}O_{\alpha c}$ values were less than 1‰ different from each other (Table 4.1). In

five of the 30 years, the $\delta^{18}O_{\alpha c}$ values were between 1-2‰ different from each other (Table 4.1). Differences of 2-3‰ were identified in four of the years and >3‰ in the six of the years (Table 4.1). Of the 10 years that had differences in $\delta^{18}O_{\alpha c}$ values of ≥2‰, seven years had below average wet season (November to April) precipitation amount. Because the annual $\delta^{18}O_{\alpha c}$ values between each chronology are, for the most part, strongly correlated, this suggests that $\delta^{18}O_{\alpha c}$ in *P. angolensis* accurately record variations in seasonal precipitation. Furthermore, these results that the Modified Brendel method is a reliable technique for alpha-cellulose extraction.

Table 4.1 Difference in $\delta^{18}O$ values per year between the two samples $\delta^{18}O_{\alpha c}$ chronology.

‰ Difference	Year
< 1‰	1955, 1957, 1960, 1966, 1967, 1972-1976, 1978, 1979, 1981-1983
1-2‰	1958, 1961, 1963, 1980, 1984
2-3‰	1956, 1964, 1968, 1970
> 3‰	1959, 1962, 1965, 1969, 1971, 1977

4.2 Ring-Width

The most significant relationships identified between ring-width and precipitation amount was during the months November through December and December alone. The correlations declined in strength when the ring-width chronology was compared to total precipitation from multiple months during the wet season, such as November to January, November to February, and November to April. This may suggest that growth of *P. angolensis* is not entirely dependent on precipitation throughout the wet season. These results are curious because Therrell et al., (2006) found a

significant correlation between ring-widths of *P. angolensis* growing in the Mzola forest and November – February precipitation amount. There are various environmental factors that can account for changes in annual ring-width, such as topography, light quality and quantity, amount of soil water, and tree productivity and health. It's very possible that the trees used in this current study grew at a different location in the Mzola forest than the trees used in the study by Therrell et al., (2006). Additionally, the sample set used in this current study is small (two trees) compared to the much larger sample set (21 trees) used in the study by Therrell et al., (2006).

The relationship between the $\delta^{18}O_{\alpha c}$ and ring-width chronologies is negative because decreased ring-width during dry conditions results in increased moisture stress, which typically leads to $^{18}O_{\alpha c}$-enriched values. Surprisingly, the ring-width chronology was only weakly correlated with the $\delta^{18}O_{\alpha c}$ chronology, which suggests that *P. angolensis* ring-width and $\delta^{18}O_{\alpha c}$ values do not represent fluctuations in precipitation in the same way. The structure and function of trees are largely influenced by water availability, particularly the periodicity and intensity of drought, and trees growing in locations with both a wet and dry season have a greater sensitivity to climate than trees growing in locations with a balanced supply of moisture year round (Abrams et al., 1998). The more limiting an environmental factor is to tree growth, the more directly variations in that factor may be related to variations in ring-width (Phipps, 1982).

Ring-width is frequently more highly correlated with drought conditions than above-average precipitation. The strongest signal I identified between the $\delta^{18}O_{\alpha c}$ chronology and precipitation amount was with above-average wet season precipitation, specifically those seasons with the highest amount of precipitation. It appears that ring-growth is more sensitive to drought conditions while $\delta^{18}O_{\alpha c}$ values are more sensitive to wet conditions. The large interannual variability in the $\delta^{18}O_{\alpha c}$ values and ring-width suggests that *P. angolensis* is sensitive to environmental and climatic

parameters and demonstrates that additional information can be gained by incorporating $\delta^{18}O_{\alpha c}$ analysis along with ring-width analysis into paleoclimate studies.

4.3 Temperature and $\delta^{18}O$

The correlations between the $\delta^{18}O_{\alpha c}$ chronology and minimum or max temperature are not significant, but are significant with mean temperature during the growing season. The strongest correlations were found with mean temperature in the months of December of the prior calendar year, the current year June, and from prior November through April. My findings are similar to past studies that also identified positive correlations between $\delta^{18}O_{\alpha c}$ and temperature (Burke and Stuiver, 1981; Raffali-Delerce et al., 2003; Ferrio and Voltas, 2005; Battipaglia et al., 2008; Kress et al. 2010; Brienen et al. 2012).

The positive correlation between the $\delta^{18}O_{\alpha c}$ chronology and wet season mean temperature could indicate an association between the direct effect of temperature on oxygen isotopic composition of meteoric water and/or the evaporative enrichment of soil water. Higher (lower) temperatures result in increased (decreased) $\delta^{18}O$ values in both meteoric water and soil water (Roden and Ehleringer, 1999; McCarroll and Loader, 2004; Daux et al., 2011). Libby et al. (1976) viewed oxygen isotopes in cellulose as "isotopic thermometers" because the oxygen isotope composition of soil water is typically linked to that of precipitation and because the oxygen isotope composition of meteoric water is known to vary with temperature. Typically, the $\delta^{18}O$ values in meteoric water are determined by the temperature of raindrop formation, increasing in enrichment with higher temperatures (Dansgaard, 1964; Ferrio and Voltas, 2005). Correlation between the annual $\delta^{18}O_{meteoric}$ data and both wet season and annual average temperatures was not significant,

implying that the temperature effect is overshadowed by the amount effect in Zimbabwe. This also suggests that the positive correlations between wet season mean temperature and the $\delta^{18}O_{\alpha c}$ chronology is a result of the evaporative enrichment of $\delta^{18}O$ in soil water. This further supports the idea that *P. angolensis* utilize soil water as opposed to ground water and that the soil water signal is recorded in the $\delta^{18}O$ ratio of cellulose.

4.4 $\delta^{18}O_{\alpha c}$ and Precipitation Amount

In tropical regions, $\delta^{18}O$ values of meteoric water are negatively correlated with wet season precipitation amount, which is a primary characteristic of intra-annual variability in the oxygen isotopic composition of meteoric water (Gat, 1996; Gagen et al., 2011). In addition to this seasonal cycle, the amount effect also embodies a climate signal: the greater the amount of precipitation during a season, the more $^{18}O_{\alpha c}$-depleted the values (Dansgaard, 1964; Gagen et al., 2011). The wet season in Zimbabwe occurs between November and April, with 80% of annual precipitation falling during the months of November to February (Therrell et al., 2006). Several past studies (Saurer, 2003; Evans and Schrag, 2004; Battipaglia et al., 2008; Kress et al., 2010; Ballantyne et al., 2011; Brienen et al., 2012) have identified negative relationships between $\delta^{18}O_{\alpha c}$ values and precipitation amount, especially in tropical locations. My findings are in agreement with those studies in that I identified significant negative relationships between wet season precipitation amount and the $\delta^{18}O_{\alpha c}$ chronology. The strongest monthly correlation between $\delta^{18}O_{\alpha c}$ and precipitation was in the month of February. Each of the wet season months (November – April) shows a declining trend in precipitation during the 30-year study period with the strongest negative trends found in both January and February (a decrease of 2 mm per year). The decreasing precipitation trend in February and the increasing trend $\delta^{18}O_{\alpha c}$ of 0.07‰ during our study period

could be indicative of the significant relationship between the $\delta^{18}O_{\alpha c}$ chronology and February precipitation amount.

Significant negative relationships were also identified when averaging November through February precipitation amount and comparing it to the $\delta^{18}O_{\alpha c}$ chronology. An even stronger relationship was found between the ten wettest years. The $\delta^{18}O_{\alpha c}$ chronology demonstrates a correlation with precipitation during the beginning of the wet season (November to December) and into the current year (January – April), implying an association with precipitation across the calendar season.

Even though seasonal temperature fluctuation is slight in Zimbabwe, the opposite is true for precipitation and I have shown through correlation analysis that $\delta^{18}O_{\alpha c}$ values in *P.* angolensis are sensitive to fluctuations in wet season precipitation amount. The relationship between the $\delta^{18}O_{\alpha c}$ values in *P. angolensis* is as follows: $^{18}O_{\alpha c}$-depletion ($^{18}O_{\alpha c}$-enrichment) of $\delta^{18}O_{\alpha c}$ values occurs in response to increases (decreases) in precipitation amount. Because of the statistical significance of this relationship, my results indicate that fluctuations in precipitation are recorded in the $\delta^{18}O_{\alpha c}$ of these tree-rings and that these parameters could be used as a possible proxy for precipitation variability in Zimbabwe.

Although $\delta^{18}O_{\alpha c}$ values record variations in precipitation amount and oxygen isotopic composition of meteoric water, Saurer et al., (2012) found that it is important to also consider atmospheric circulation in extracting information from the isotope signal in tree rings. Through their research, it was observed that on average high-pressure situations during summer were associated with relatively ^{18}O-enriched values and low-pressure situations were associated with relatively ^{18}O-depleted values, for both the isotope ratio in precipitation and tree rings. This may be partly an explanation for the attenuated correlations that I identified between precipitation

amount $\delta^{18}O_{\alpha c}$ during the November through January wet season months, as only the month of February was statistically significantly correlated with the $\delta^{18}O_{\alpha c}$ chronology. Kress et al., (2010) determined that $\delta^{18}O_{\alpha c}$ values accurately record oxygen isotopic composition of meteoric water, which in turn depends heavily on the origin of the air masses. Regions more frequently subjected to air masses of the same origin are more likely to exhibit stronger climate-isotope relationships as opposed to regions that are characterized by a more complex synoptic situation. Air masses with heterogeneous origins during the growing season may influence the $\delta^{18}O_{\alpha c}$ signature, resulting in weaker correlations with temperature and precipitation amount (Kress et al., 2010). SST patterns in the eastern Atlantic and western Indian Oceans influence precipitation variability over much of southern Africa (Nicholson, 2001) and the air masses originating over both these locations will be composed of water vapor with distinct $\delta^{18}O$ values. Based on the conclusions made by Kress et al. (2010), the fact that precipitation amount and $\delta^{18}O_{\alpha c}$ values are only significantly correlated with the month of February in this study may be the result of different origins of air masses that transport water vapor to southern Africa.

4.5 Meteoric Water

Past studies have found significant positive correlations between $\delta^{18}O_{\alpha c}$ and $\delta^{18}O_{meteoric}$ values (Burk and Stuiver, 1981; Anderson et al., 1998; Saurer et al., 2000; Evans and Schrag, 2004; Anchukaitis et al., 2008). The correlations I identified between these variables are also highly significant even with small sample sizes (n = 17-20). The source of water for trees is soil moisture, and the $\delta^{18}O_{\alpha c}$ signal will vary linearly with the oxygen isotope composition in meteoric water (Roden and Ehleringer, 1999; McCarroll and Loader, 2004).

There are several potential fractionations that can occur before $\delta^{18}O$ becomes fixed in alpha-cellulose and the oxygen isotopic composition of unsaturated soil water utilized by tree roots can be affected by evaporation, groundwater depth, and residence time (McCarroll and Loader, 2004; State Key Laboratory of Hydrology-Water Resources and Hydraulic Engineering). Due to the influence of soil depth on meteoric water, the oxygen isotopic composition of groundwater is representative of seasonal precipitation, has less variation (in heavy to light $\delta^{18}O$), and represents the long-term mean of the $\delta^{18}O$ values of meteoric water (Allison et al, 1983; Saurer et al., 1997; Fig. 1.10).

White et al., (1985), measured sap from trunks of white *Pinus strobus* (white pine), and determined that the isotopic enrichment of sap water is controlled by the amount of groundwater accessible to the tree and trees that lacked access to groundwater reflected the Deuterium isotope (δD) composition of precipitation. Like $\delta^{18}O$, δD values can be measured precipitation and vary seasonally**.** Hartsough et al., (2008) showed that *Pinus hartwegii* (Hartweg's pine) growing in dry sites with a prolonged dry season utilize water from relatively shallow depths, which is representative of current precipitation conditions, and that groundwater, which is more representative of long-term precipitation trends, does not contribute to the source water.

Though *P. angolensis* has an extensive root system, meteoric water at the study site will presumably drain quickly through the Kalahari sand, as the physical properties of sand do not provide for vertical mixing of groundwater. Root depth can also affect the $\delta^{18}O_{\alpha c}$ values of tree-rings, as deeply rooted trees that can access groundwater will be taking in a mixture of ^{18}O-enriched and ^{18}O-depleted meteoric water from combined "old" precipitation and "new" precipitation (Song et al., 2010). Shallow-rooting trees may maintain a stronger record of annual variations in the $\delta^{18}O$ of meteoric water (McCarroll and Loader, 2004). It can therefore be

hypothesized that *P. angolensis* roots take in water from an unsaturated zone, as the pores in the sand will not be filled with water. The positive relation between the $\delta^{18}O_{\alpha c}$ chronology and $\delta^{18}O_{meteoric}$ values suggested minimal utilization of groundwater of the previous summer and previous year by *P. angolensis* (e.g., Rinne et al., 2013).

4.6 Isotopic Amount Effect

Above average monthly or annual precipitation amount typically leads to $^{18}O_{meteoric}$-depleted values, a phenomenon known as the "amount effect" (Dansgaard, 1964). The oxygen isotopic composition of meteoric water can leave a signature in wood constituents, such as alpha-cellulose, as trees take up soil water through their roots. To test whether an isotopic amount effect existed, I compared the $\delta^{18}O_{meteoric}$ values to seasonal precipitation amount. I tested the amount effect on monthly time scales and found that the strongest negative correlation is with January precipitation totals. I identified a significant negative correlation between increases in precipitation and $\delta^{18}O_{meteoric}$ - depleted values in the months of November through February. As expected, my results suggest that the amount effect is present in the $\delta^{18}O$ signature of meteoric water. My results confirm the notion that above (below) average amounts of precipitation result in $^{18}O_{meteoric}$-depleted values ($^{18}O_{meteoric}$-enriched values).

Past studies have identified positive relationships between $\delta^{18}O_{\alpha c}$ values and $\delta^{18}O_{meteoric}$ values (Burk and Stuiver, 1981; Saurer et al., 2002; Evans and Schrag, 2004; Brienen et al., 2012). The strongest relationship I identified was between November through January $\delta^{18}O_{meteoric}$ values and the $\delta^{18}O_{\alpha c}$ chronology. I identified a significant positive relationship between the $\delta^{18}O_{\alpha c}$ chronology and annual $\delta^{18}O_{meteoric}$ values, which suggests that variations in $\delta^{18}O_{\alpha c}$ values are related to variations in $\delta^{18}O_{meteoric}$ inputs. It's possible that the positive correlation between precipitation

amount and the $\delta^{18}O_{\alpha c}$ chronology occurred from the covariance of precipitation amount and $\delta^{18}O_{meteoric}$ values (Roden et al., 2005).

The $\delta^{18}O_{\alpha c}$ chronology reveals larger annual amplitude (range of 14.7‰) compared to the annual $\delta^{18}O_{meteoric}$ values (range of 5.1‰). The increased variability of $\delta^{18}O_{\alpha c}$ values may be the result of the two *P. angolensis* trees taking in surface water as opposed to groundwater. If the trees were relying on groundwater, the $\delta^{18}O$ signal should be more homogenous and there would likely be less annual variation in $\delta^{18}O_{\alpha c}$ values.

4.7 Relationship between SST and $\delta^{18}O_{\alpha c}$ Values

Anomalous SSTs are associated with positive and negative ENSO events, which affect interannual variability in precipitation throughout much of the tropics, including southern Africa. Past research has identified significant negative correlations between ENSO events, decreased precipitation, and $^{18}O_{\alpha c}$-enriched values in tree-rings (Nicholson, 2001; Poussart et al., 2004; Anchukaitis and Evans, 2010; Ballantyne et al., 2011; Xu et al., 2011; Brienen et al., 2012). The positive and negative precipitation anomalies in southern Africa associated with an ENSO cycle correspond to cold and warm phases in the adjacent Atlantic and Indian Oceans (Nicholson and Kim, 1997). Typically in southern Africa, precipitation tends to be enhanced during the cold La Niña phase, leading to $^{18}O_{\alpha c}$-depleted values and reduced during the warm El Niño phase, leading to $^{18}O_{\alpha c}$-enriched values. Nicholson (2001) determined that the ENSO signal in precipitation variability over southern Africa occurs in response to specific patterns of SSTs in the Atlantic and Indian Oceans surrounding Africa, which develop in approximately three out of four ENSO events.

Therefore, the main control on precipitation in this region may be SSTs in the western Atlantic and Eastern Indian Oceans, as opposed to ENSO itself (Nicholson, 2001).

Composite analysis of seasonal (November – February) SSTs for the five most $^{18}O_{ac}$-depleted values (Fig. 3.14) and the five most $^{18}O_{ac}$-enriched values (Fig. 3.15) in the 30-year chronology may suggest an ENSO influence on $\delta^{18}O_{ac}$ values of *P. angolensis* in Zimbabwe. In figure 3.14, cold anomalies are visible in the southeastern equatorial Atlantic Ocean, southwestern equatorial Indian Ocean, and, most notably, in the South Pacific Ocean, corresponding to La Niña conditions. All but one of these years (1959) experienced well-above average precipitation during the wet season (November to April). Moisture from the Atlantic and Indian Oceans, in response to cold SST anomalies, transported to Zimbabwe will be heavy in $H_2O^{18}O$ isotopologues and may blur the isotopic amount effect signal often observed in the tropics. Though, there appears to be a corresponding signal in $\delta^{18}O_{ac}$ to both negative SST anomalies and above average wet season precipitation amount.

In Fig. 3.15, warm anomalies are visible in the south Pacific and Indian Oceans. Only one of the five years experienced below-average wet season precipitation amount (1962). Moisture from the Atlantic and Indian Oceans, in response to warm SST anomalies, will contain less $H_2O^{18}O$ isotopologues. The ^{18}O-depleted moisture transported into Zimbabwe could possibly be blurring the isotopic amount effect, leading to weak correlations between years of below-average precipitation and $^{18}O_{ac}$-enriched values.

These results may indicate that SST in the Atlantic, Indian, and Pacific Oceans is an important factor in regulating the $\delta^{18}O$ values of precipitation over southern Africa. Additionally, further analysis would need to be performed in order to determine whether it is actually large-scale

atmospheric circulation that is controlling the $\delta^{18}O_{\alpha c}$ values in *P. angolensis* and not the result of a local amount effect (Brienen et al., 2012).

CHAPTER 5

CONCLUSION

The results of this study provide evidence that $\delta^{18}O$ in the alpha-cellulose of *P. angolensis* capture variability in precipitation amount, $\delta^{18}O$ values of meteoric water, and mean temperature. By analyzing inter-annual variability in the $\delta^{18}O_{\alpha c}$ values, I have shown that $\delta^{18}O_{\alpha c}$ values fluctuate on annual timescales and that the fluctuations correspond most strongly with wet season precipitation patterns. The amplitude of the annual cycle of $\delta^{18}O_{\alpha c}$ could potentially be used to estimate seasonal precipitation amounts in western Zimbabwe prior the instrumental record and could possibly be useful in determining the seasonal response of tropical trees that that lack annual growth rings. The $\delta^{18}O_{\alpha c}$ values are negatively correlated with seasonal precipitation, which is consistent with the isotopic amount effect control on $\delta^{18}O_{\alpha c}$ values. I find it remarkable that analyzing the $\delta^{18}O_{\alpha c}$ values from only two trees produces fairly strong climate signals, especially when correlated to wet season precipitation amount.

The results of this study also suggest that annual $\delta^{18}O_{\alpha c}$ values from *P. angolensis* may be sensitive to precipitation variability dominated by SST anomalies in the Atlantic and Indian Oceans. Annual variations in $\delta^{18}O_{\alpha c}$ values of *P. angolensis* appear to be a mixture of local effects (e.g., amount effect) and large-scale influences (e.g., variation in the $\delta^{18}O$ signature during moisture transport to Zimbabwe) (Brienen, et al., 2012). It is possible that the $\delta^{18}O$ signature in precipitation and meteoric water reflects the $\delta^{18}O$ signature in moisture as it is transported from the Atlantic and Indians Oceans, rather than a local isotopic amount effect (Brienen et al., 2012).

By investigating the annual $\delta^{18}O_{\alpha c}$ values and ring-widths in *P. angolensis*, I found that ring-width is correlated with precipitation amount but has a different response to precipitation than

$\delta^{18}O_{\alpha c}$. Ring-width data typically show a pattern to drought occurrences and our results suggest that $\delta^{18}O_{\alpha c}$ show a pattern to well-above average precipitation. Because ring-width is more responsive to drought years and $\delta^{18}O_{\alpha c}$ to wet years, combining both proxies, as opposed to using each one independently, may be more effective in paleoclimate studies. These results are promising and indicate that it may be possible to extend the instrumental precipitation records for Zimbabwe using multiple proxies from *P. angolensis*.

Correlation analysis between the $\delta^{18}O_{\alpha c}$ chronology and seasonal precipitation constitute a response function that can possibly help to identify how variations in climate are related to variations in $\delta^{18}O_{\alpha c}$, though additional work still needs to be carried out in order for *P. angolensis* to be used as a proxy for paleoclimate studies. Utilizing a larger sample set and extending the $\delta^{18}O_{\alpha c}$ chronology from *P. angolensis* should increase the utility of this study and provide more precise estimates of past spatial and temporal precipitation variability in Zimbabwe. As the first $\delta^{18}O_{\alpha c}$ proxy record developed from tree rings in southern Africa, this study has provided the framework for future analysis of precipitation variability over this region and has contributed to isotope dendro-paleoclimatology in the tropics.

REFERENCES

Abrams, M., C. Ruffner, and T. Morgan. 1998. Tree Ring Responses to Drought Across Species and Contrasting Sites in the Ridge and Valley of Central Pennsylvania. *The Society of American Foresters* 44: 550-558.

Allison, G. B., C. J. Barnes, and M. W. Hughes. 1983. The Distribution of Deuterium and ^{18}O in Dry Soils. *Journal of Hydrology* 64: 377-397.

An, W., et al. 2012. Specific Climatic Signals Recorded in Earlywood and Latewood $\delta^{18}O$ of Tree Rings in Southwestern China. *Tellus B* 64. http://www.tellusb.net/index.php/tellusb/article/view/18703/html

Anchukaitis, K. J., et al. 2008. Consequences of a Rapid Cellulose Extraction Technique for Oxygen Isotope and Radiocarbon Analysis. *Journal of Geophysical Research* 113: 1-17.

Anchukaitis, K., and M. Evans. 2010. Tropical Cloud Forest Climate Variability and the Demise of the Monteverde Golden Toad. *Proceedings of the National Academy of Sciences* 107 (March), http://www.pnas.org/content/107/11/5036.long.

Anderson, W. T., S. M. Bernasconi, and J. A. McKenzie. 1998. Oxygen and Carbon Isotopic Record of Climatic Variability in Tree Ring Cellulose (*Picea abies*): An Example of Central Switzerland (1973-1995). *Journal of Geophysical Research* 103: 31,625-31,636.

Bale, R., et al. 2010. Temporal Stability in Bristlecone Pine Tree-Ring Stable Oxygen Isotope Chronologies Over the Last Two Centuries. *The Holocene*, 3-6.

Ballantyne, A. P., et al. 2011. Regional Differences in South American Monsoon Precipitation Inferred from the Growth and Isotopic Composition of Tropical Trees. *Earth Interactions* 15.5 1-35.

Barbour, M., et al. 2004. Expressing Leaf Water and Cellulose Oxygen Isotope Ratios as Enrichment Above Source Water Reveals Evidence of a Péclet Effect 138: 426-435.

Battipaglia, G., et al. 2008. Climatic Sensitivity of $\delta^{18}O$ in the Wood and Cellulose of Tree Rings: Results from a Mixed Stand of *Acer pseudoplatanus* L. and *Fagus sylvatica* L. *Palaeogeography, Palaeoclimatology, Palaeoecology* 261: 193-202.

Boko, M., et al. 2007. Impacts, Adaptation and Vulnerability. Contribution of Working Group II to the Fourth Assessment Report of the Intergovernmental Panel on Climate Change. Cambridge University Press, Cambridge UK, 433-467.

Bowen, G. J. 2008. Spatial Analysis of the Intra-Annual Variation of Precipitation Isotope Ratios and its Climatological Corollaries. *Journal of Geophysical Research* 113: (March). http://wateriso.eas.purdue.edu/waterisotopes/media/PDFs/Precip_Seasonality.pdf

Brendel, O., P. P. M. Iannetta, and D. Stewart. 2000. A Rapid and Simple Method to Isolate Pure Alpha-cellulose. *Phytochemical Analysis* 11.1: 7-10.

Brook, G. A., et al. 1999. A High-Resolution Proxy Record of Rainfall and ENSO Since AD 1550 from Layering in Stalagmites from Anjohibe Cave, Madagascar. *The Holocene* 9: 695-705.

Burke, R. L., and M. Stuiver. 1981. Oxygen Isotope Ratios in Trees Reflect Mean Annual Temperature and Humidity. *Science* 211: 1417-1419.

Cook, E. 1990. *Methods of Dendrochronology.* Dordrecht, Holland: Kluwer Academic Publishers.

Coplen, T. B., A. L. Herczeg, C. Barnes. 2000. Isotope Engineering-Using Stable Isotopes of the Water Molecule to Solve Practical Problems. Environmental Tracers in Subsurface Hydrology, 79-110.

Dansgaard, W. 1964. Stable Isotopes in Precipitation. *Tellus* 16(4): 436-467.

Daux, V., et al. 2011. Can Climate Variations be Inferred from Tree-Ring Parameters and Stable Isotopes from *Larix decidua*? Juvenile Effects, Budmoth Outbreaks, and Divergence Issue. *Earth and Planetary Science Letters* 309: 221-233.

DeNiro, M. J., and S. Epstein. 1979. Relationship between the oxygen isotope ratios of terrestrial plant cellulose, carbon dioxide, and water. ^{18}O, ^{16}O. *Science* 204: 51-53.

Dunwiddie, P. W., and V. LaMarche. 1980. A Climatologically-Responsive Tree-Ring Record from Widdringtonia Cedarbergensis, Cape Province, South Africa. *Nature* 286: 796-797.

Dyson, L. and J. van Heerden. 2001. The Heavy rainfall and Floods Over the Northeastern Interior of South Africa During February 2000. *South African Journal f Science* 93: 80-86.

Ellis, F., M. Kutemgule, and A. Nyasulu. 2003. Livelihoods and Rural Poverty Reduction in Malawi. *World Development* 31: 1945-1510.

Evans, M. N., and D. Schrag. 2003. Tracking ENSO with Tropical Trees: Progress Using Stable Isotope Dendroclimatology. *Geochimica et Cosmochimica Acta* 68: 3295–3305.

Evans, M. N., and D. Schrag. 2004. A Stable Isotope-Based Approach to Tropical Dendroclimatology. *Geochimica et Cosmochimica Acta* 66: 3295-3305.

Fauchereau, N., et al. 2003. Rainfall Variability and Changes in Southern Africa during the 20th Century in the Global Warming Context. *Natural Hazards* 29: 139-154.

Ferrio, J. P., and J. Voltas. 2005. Carbon and Oxygen Isotope Ratios in Wood Constituents of *Pinus halepensis* as Indicators of Precipitation, Temperature and Vapour Pressure Deficit. *Tellus* 57B: 164-173.

Fichtler, et al. 2004. Climatic Signals in Tree Rings of *Burkea Africana* and *Pterocarpus angolensis* from Semiarid Forests in Nambia. *Trees.* 18: 442-451.

Fitzsimons, I. C. W., B. Harte, and R. M. Clark. 2000. *Mineralogical Magazine* 64: 59-83.

Gagen, M., et al. 2011. Stable Isotopes in Dendroclimatology: Moving Beyond 'Potential'. *Developments in Paleoenvironmental Research* 11: 147-172.

Gat, J. R., and R. Gonfiantini. 1981. *Stable Isotopes Hydrology; Deuterium and Oxygen-18 in the Water Cycle*. Vienna, International Atomic Energy Agency, Technical Reports 210.

Gat, J. R. 1996. Oxygen and Hydrogen Isotopes in the Hydrologic Cycle. *Annual Review of Earth and Planetary Sciences* 24: 225-262.

Gaudinski, J. B., et al. 2005. Comparative Analysis of Cellulose Preparation Techniques for Use with C, H, and O Isotopic Measurements. *Analytical Chemistry* 77.22: 7212-224.

Grootes, P. M., et al. 1989. Rapid Response of Tree Cellulose Radiocarbon Content to Changes in Atmospheric $^{14}C0_2$ Concentration. *Tellus* 41: 134-148.

Grove, C. A., et al. 2012. Madagascar Corals Reveal Pacific Multidecadal Modulation of Rainfall Since 1708. *Climate of the Past Discussions* 8: 787-817.

Hartsough, P., et al. 2008. Stable Isotope Characterization of the Ecohydrological Cycle at a Tropical Treeline Site. *Arctic, Antarctic, and Alpine Research* 40: 343-354.

Hsieh et al. (1998) Oxygen Isotopic Composition of Soil Water: Quantifying Evaporation and Transpiration. *Geoderma* 82: 269-293.

Hoefs, J. 1997. *Stable Isotope Geochemistry*. Berlin: Springer.

Holmgren, K., et al. 2001. A Preliminary 3000-Year Regional Temperature Reconstruction for South Africa. *South African Journal of Science* 97: 49-51.

Horan , P.D. 2011. "Exploring Seasonal Climate Variability in East African Trees: High-Resolution Oxygen and Carbon Isotope Records of Cellulose of *Vitex payos* from Chyulu Hills, Kenya." (Masters Thesis, University of Southern California).

Hulme, M., et al. 2001. African Climate Change. *Climate Research* 17: 145-168.

International Atomic Energy Agency. Global Network of Isotopes in Precipitation. http://www-naweb.iaea.org/napc/ih/IHS_resources_gnip.html

Kinsey, B., K. Burger, and J. W. Gunning. Coping with Drought in Zimbabwe: Survey Evidence on Responses of Rural Households to Risk. *World Development* 26: 89-110.

Kress, A., et al. 2009b. Stable Isotope Coherence in the Earlywood and Latewood of Tree- Line Conifers. *Chemical Geology* 268: 52–57.

Kress, A., et al. 2010. A 350 year drought reconstruction from Alpine tree ring stable isotopes. *Global Biogeochemical Cycles* 24: 1-16.

Le Quense, C., et al. 2006. Ancient *Austrocedrus* Tree-Ring Chronologies Used to Reconstruct Central Chile Precipitation Variability from A.D. 1200 to 2000. *Journal of Climate* 19: 5731-5743.

Lee-Thorp, J.A., et al. 2001. Rapid Climate Shifts in the Southern African Interior Throughout the Mid to Late Holocene. *Geophysical Research Letters* 28: 4507-4510.

Lee, J., and I. Fung. 2008. Amount Effect of Water Isotopes and Quantitative Analysis of Post-condensation Processes. *Hydrological Processes* 22.1: 1-8.

Leichenko, R. and K. L. O'Brien. 2001. The Dynamics of Rural Vulnerability to Global Change: The Case of Southern Africa. *Mitigation and Adaptation Strategies for Global Change* **7:** 1–18

Li, J., et al. 2006. Tree-ring based drought reconstruction for the central Tien Shan area in northwest China. *Geophysical Research Letters* 33 (April). http://onlinelibrary.wiley.com/doi/10.1002/grl.v33.7/issuetoc.

Li, Z., et al. 2011. Micro-scale Analysis of Tree Ring $\delta^{18}O$ and $\delta^{13}C$ on α-cellulose Spline Reveals High-resolution Intra-annual Climate Variability and Tropical Cyclone Activity. *Chemical Geology* 284: 138-47.

Liang, E., X. Shao, and N. Qin. 2008. Tree-ring based summer temperature reconstruction for the source region of the Yangtze River on the Tibetan Plateau. *Global and Planetary Change* 61:313-320.

Libby, L. M., and L. J. Pandolfi. 1974. Temperature Dependence of Isotope Ratios in Tree Rings. *Proceedings of the National Academy of Sciences of the United States of America* 71: 2482-2486.

Libby, L. M., et al, 1976. Isotopic Tree Thermometers. *Nature* 261: 284-290

Liu, Y., et al. 2008. Monsoon Precipitation Variation Recorded by Tree-Ring $\delta^{18}O$ in arid Northwest China since AD 1878. *Chemical Geology* 252: 56-61.

Loader, N. J., et al. 1997. An Improved Technique for the Batch Processing of Small Wholewood Samples to α-cellulose. *Chemical Geology* 136.3-4: 313-17.

Makarau, A., and M. R. Jury. 1997. Predictability of Zimbabwe Summer Rainfall. *International Journal of Climatology* 17.13: 1421-432.

Managave, S.R. and R. Ramesh. 2011. Isotope Dendroclimatology: A Review with a Special Emphasis on Tropics. In Handbook of Environmental Isotope Geochemistry, Advances in Isotope Geochemistry, ed. M. Baskaran. Springer-Verlag- Berlin Heidelberg. Chapter 38: 811-833.

Manatsa, D., et al. 2010. Analysis of Multidimensional Aspects of Agricultural droughts in Zimbabwe Using Standardized Precipitation Index (SPI). *Theoretical and Applied Climatology* 102: 287-305.

McCarroll, D., and N. J. Loader. 2004. Stable Isotopes In Tree Rings. *Quaternary Science*. 23: 771-801.

McCarroll, D., and N. J. Loader. 2005. Isotopes in Tree Rings. *Isotopes in Paleoenvironmental Research* 10:67-116.

Mushove, P., Stahle, D. W., and M. K. Cleaveland, 1997. IGBP PAGES/World Data Center for Paleoclimatology Data Contribution # ZIMB002, Mzola Forest. NOAA/NCDC Paleoclimatology Program, Boulder, Colorado, USA.

Nash, D. J. 2008. Splendid Rains Have Fallen': Links Between El Nino and Rainfall Variability in the Kalahari, 1840-1900. *Climate Change* 86: 257-290.

National Aeronautics and Space Administration (NASA). Climate Science Investigations: South Florida. http://131.91.162.18/nasa/module-3/how-is-temperature-measured/isotopes.

National Oceanic and Atmospheric Administration (NOAA). National Climatic Data Center/Paleoclimatology: Tree-Ring Database. http://www.ncdc.noaa.gov/paleo/treering.html.

Nicholson, S. E. 1981. Rainfall and Atmospheric Circulation During Drought Periods and Wetter Years in West Africa. *American Meteorological Society* 109: 2191-2208.

Nicholson, S. E. 1986. A Spatial Coherence of African Rainfall Anomalies: Interhemispheric Teleconnections. *Journal of Climate and Applied Meteorology* 25: 1365-1381.

Nicholson, S. E. 1987. Rainfall Variability in Equatorial and Southern Africa: Relationships with Sea Surface Temperatures along the Southwestern Coast of Africa. *Journal of Climatology and Applied Meteorology* 26: 561-578.

Nicholson, S., and J. Kim. 1997. The Relationship of the El Niño-Southern Oscillation to African Rainfall. *International Journal of Climatology* 17: 117-135.

Nicholson, S. E. 1999. African Drought: Characteristics, Causal Theories and Global Teleconnections. *Geophysical Monograph Series* 52: 79-100.

Nicholson, S. E. 2000. The Nature of Rainfall Variability over Africa on Time Scales of Decades to Millenia. *Global and Planetary Change* 26: 137-158.

Nicholson. S. E. 2001. Climatic and Environmental Change in Africa During the Last Two Centuries. *Climate Research* 17: 123-144.

Nkomozepi, Y. and S. Chung, 2012. Assessing the Trends and Uncertainty of Maize Net Irrigation Water Requirement Estimated From Climate Change Projections for Zimbabwe. *Agricultural Water Management* 111: 60-67.

Phipps, R. L. 1982. Comments on Interpretation of Climatic Information from Tree Rings, Easter North America. *Tree Ring Bulletin* 42: 11-22

Poussart. P. F., M. N. Evans, and D. P. Schrag. 2004. Resolving Seasonality in Tropical Trees: Multi-Decade, High-Resolution Oxygen and Carbon Isotope Records from Indonesia and Thailand. *Earth and Planetary Science Letters* 218: 301-316.

Raffali-Delerce, G., et al. 2004. Reconstruction of Summer Droughts Using Tree-Ring Cellulose Isotopes: A Calibration Study with Living Oaks from Brittany (Western France). *Tellus* 56B: 160-174.

Rebetez, M., M. Saurer, and P. Cherubini. 2003. To What Extent Can Oxygen Isotopes in Tree Rings and Precipitation be Used to Reconstruct past Atmospheric Temperature? A Case Study. *Climatic Change* 61: 237-48.

Rinne, K. T. 2005. On the Purification of Alpha Cellulose from Resinous Wood for Stable Isotope (H,C,O) Analysis. *Chemical Geology* 222: 75-82.

Rinne, K. T., et al. 2013. 400-Year May–August Precipitation Reconstruction for Southern England Using Oxygen Isotopes in Tree Rings. *Quaternary Science Reviews* 60: 13-25.

Robertson, I., et al. 2001. Oxygen Isotope Ratios of Oak in East England: Implications for Reconstructing the Isotopic Composition of Precipitation. *Earth and Planetary Science Letters* 191: 21-31.

Roden, J. S., G. Lin, J. Ehleringer. 1999. Observations of Hydrogen and Oxygen Isotopes in Leaf Water Confirm the Craig-Gordon Model under Wide-Ranging Environmental Conditions. *Plant Physiology* 120: 1165-1173.

Roden, J. S., G. Lin, J. Ehleringer. 2000. A Mechanistic Model for Interpretation of Hydrogen and Oxygen Isotope Ratios in Tree-Ring Cellulose. *Geochimica et Cosmoshimica* 64: 21-35.

Roden, J. S., et al. 2005. Carbon and Oxygen Isotope Ratios of Tree Ring Cellulose Along a Precipitation Transect in Oregon, United States, *Journal of Geophysical Research* 110 (October). http://andrewsforest.oregonstate.edu/pubs/pdf/pub4118.pdf.

Roden, J. S., J. A. Johnstone, and T. E. Dawson. 2011. Regional and Watershed-scale Coherence in the Stable Oxygen and Carbon Isotope Ratio Time Series in Tree Rings of Coast Redwood. *Tree-Ring Research* 6.2: 71-86.

Rouault, Mathieu. 2005. Intensity and Spatial Extent of Droughts in Southern Africa. *Geophysical Research Letters* 32: 1-4.

Rozanski, K., L. Araguas, R. Gonfiantini. 1993. Isotopic patterns in modern global precipitation. *Geophysical Monograph Series* 78: 1-36.

Saurer, M., K. Aellen, and R. Siegwolf. 1997. Correlating $\delta^{13}C$ and $\delta^{18}O$ in Cellulose of Trees. *Plant, Cell, and Environment* 20: 1543-1550.

Saurer, M., P. Cherubini, and R. Siegwolf. 2000. Oxygen Isotopes in Tree Rings of *Abies alba*: The Climatic Significance of Interdecadal Variations. *Journal of Geophysical Research* 105: 12,461-12,470.

Saurer, M., et al. 2002. Spatial and Temporal Oxygen Isotope Trends at the Northern tree-line in Eurasia. *Geophysical Research Letters* 29: 10-13.

Saurer, M. 2003. The Influence of Climate on the Oxygen Isotopes in Tree-Rings. *Isotopes in Environment and Health Studies* 39: 105-112.

Saurer, M., et al. 2012. Influence of Atmospheric Circulation Patterns on the Oxygen Isotope Ratio of Tree Rings in the Alpine Region. *Journal of Geophysical Research* 117 (March). http://onlinelibrary.wiley.com/doi/10.1029/2011JD016861/abstract.

Schweingruber, F. 1989. *Tree Rings.* Dordrecht, Holland: Kluwer Academic Publishers.

Shackleton, C. M., and I. Adelfang, 1992. An Appraisal of Attitudes of Craft Retailers in the Eastern Transvaal Lowveld: Suggestions for Handicraft Producers in Mhala. Unpublished Report. Wits Rural Facility, Acornhoek.

Shackleton, C.M. 2002. Growth patterns of *Pterocarpus angolensis* in savannas of the South African lowveld. *Forest Ecology and Management* 166: 1-3.

Sharp, Z. 2007. *Stable Isotope Geochemistry*. Upper Saddle River, NJ: Pearson Education.

Shongwe, M.E., et al. 2009. Projected Changes in Mean and Extreme Precipitation in Africa under Global Warming. Part 1: Southern Africa. *American Meteorlogical Society* 22: 3819-3837.

Sithole, Alec and C. T. F. Murewi. 2009. Climate Variability and Change Over Southern Africa: Impacts and Challenges. *Ecology* 47: 17-20.

Song, X., et al. 2011. Relationships between Precipitation, Soil Water and Groundwater at Chongling Catchment with the Typical Vegetation Cover in the Taihang Mountainous Region, China. *Environmental Earth Sciences* 62: 787-796.

Stahle, David W. 1997. Development of a Rainfall Sensitive Tree-Ring Chronology in Zimbabwe. *American Meteorology Society*, 1-7.

Stahle, D.W., et al. 1999. Management Implications of Annual Growth Rings in *Pterocarpus angolensis* from Zimbabwe. *Forest Ecology and Management* 124: 217-229.

Nanjing Hydraulic Research Institute. State Key Laboratory of Hydrology-Water Resources and Hydraulic Engineering. Study on The Unsaturated Soil Water Extracting for Stable Isotope. http://www.seiofbluemountain.com/upload/product/201002/12657672721dzdi3fc. pdf.

Sternberg, L. 2008. Oxygen Stable Isotope Ratios of Tree-Ring Cellulose: the Next Phase of Understanding. *New Phytologist* 181: 553-562.

Stokes, M. A., and T. L. Smiley. 1996. An introduction to tree ring dating. Arizona Przess, Tucson.

Stringer, L. et al. 2009. Adaptations to Climate Change, Drought and Desertification: Local Insights to Enhance Policy in Southern Africa. *Elsevier* 12: 748-765.

Switsur, R., and J. Waterhouse. 1998. Stable Isotopes in Tree Ring Cellulose. *Stable Isotopes: Integration of Biological, Ecological and Geochemical Processes*. Oxford, UK: BIOS Scientific, 303-21.

Tang, K., and Feng, X. 2001. The Effect of Soil Hydrology on the Oxygen and Hydrogen Isotopic Compositions of Plants' Source Water. *Earth and Planetary Science Letters* 185: 355-367.

Therrell, M., et al. 2006. Tree-Ring Reconstructed Rainfall Variability in Zimbabwe. *Climate Dynamics* 26: 677-685.

Therrell, M., et al. 2007. Age, and Radial Growth Dynamics of *Pterocarpus angolensis* in Southern Africa. *Forest Ecology and Management* 244: 24-31.

Thompson, L.G. 2002. Kilimanjaro Ice Core Records: Evidence of Holocene Climate Change in Tropical Africa. *Science* 298: 589-593.

Unganai, L. 1996. Historic and Future Climate Change in Zimbabwe. *Climate Research* 6: 137-145.

United Nations Environment Programme (UNEP). 2009. Droughts and Floods in Southern Africa: Environmental Change and Human Vulnerability. *The Division of Early Warning and Assessment* (UNEP, SARDC), 9-44.

United States Department of Energy. Chemical Sciences, Geosciences, & Biosciences (CSGB) Division. http://agg.pnnl.gov/docs/conducting-work/ex22.stm.

University of East Anglia, Norwich, UK. Climate Research Unit. http://www.cru.uea.ac.uk/data.

Usman, M. and C, J, C, Reason. 2004. Dry spell frequencies and their variability over southern Africa. *Climate Research.* 26: 199-211.

Verschuren, D. 2004. Decadal and Century-Scale Climate Variability in Tropical Africa During the Past 2000 Years. *Past Climate Variability through Europe and Africa*. Kluwer. Academic Publishers, Dordrecht, The Netherlands, 139-158.

Von Breitenbach, F. 1973. *Pterocarpus angolensis* a Monograph. Trees in South Africa. *Journal of the Tree Society of Southern Africa* 25: Part 3.

Vuille, M., et al. 2003. Modeling $\delta^{18}O$ in Precipitation Over the Tropical Americas: 2. Simulation of the Stable Isotope Signal in Andean Ice Cores. *Journal of Geophysical Research* 108: 4175-4192.

Vuille, M., et al.. 2005. Stable Isotopes in East African Precipitation Record Indian Ocean Zonal Mode. *Geophysical Research Letters* 32: Print.

White, J., et al. 1985. The D/H Ratios of Sap in Trees: Implications for Water Sources and Tree Ring D/H Ratios. *Geochemica et Cosmochimica Acta* 49: 237-246.

Xu, C., M. Sano, and T. Nakatsuka. 2011. Tree Ring Cellulose $\delta^{18}O$ of *Fokienia hodginsii* in Northern Laos: A Promising Proxy to Reconstruct ENSO? *Journal of Geophysical Research* (December). http://onlinelibrary.wiley.com/doi/10.1029/2011JD016694/abstract**.**

Zinke, J. 2009. Western Indian Ocean marine and terrestrial records of climate variability: a review and new concepts on land-ocean interactions since AD 1660. *International Journal of Earth Science* 98: 115-133.

APPENDIX

Table 2.1: Ring-width data for samples MZO30 and MZO35 for the period 1955-1984.

Year	MZO30 Ring-Width (mm)	MZO35 Ring-Width (mm)
1955	2.202	2.339
1956	0.947	0.728
1957	1.487	2.285
1958	0.314	1.455
1959	0.665	1.632
1960	1.805	1.109
1961	0.909	2.236
1962	1	2.26
1963	1.68	2.432
1964	1.152	1.773
1965	1.165	1.661
1966	1.777	1.82
1967	2.032	1.298
1968	0.841	0.535
1969	0.492	0.842
1970	1.425	3.3
1971	1.767	1.215
1972	1.229	1.149
1973	0.707	0.828
1974	1.794	1.916
1975	0.799	2.571
1976	0.966	1.507
1977	1.072	1.763
1978	1.327	2.016
1979	1.068	1.38
1980	3.067	2.277
1981	1.501	1.75
1982	1.285	2.374
1983	0.699	0.854
1984	0.409	0.554

Table 2.2 Ring-width data for samples MZO30 and MZO35.

	MZO30	**MZO35**	**Average Width**
Age	1894-1997	1989-1997	
Ring size (mm)			
Min	0.31	0.53	0.48
Max	3.07	3.3	2.67
Mean	1.25	1.66	1.46

Table 3.1 $\delta^{18}O_{\alpha c}$ data for samples MZO30, MZO35, and the average $\delta^{18}O_{\alpha c}$ values of both samples.

	$\delta^{18}O$ (‰)		
Year	**MZO30**	**MZO35**	**Average**
1955	25.58	25.87	25.73
1956	27.25	24.48	25.87
1957	28.55	29.31	28.93
1958	25.32	23.68	24.50
1959	21.04	28.47	24.75
1960	26.68	26.90	26.79
1961	30.03	31.07	30.55
1962	31.22	35.24	33.23
1963	29.12	30.95	30.04
1964	26.17	29.13	27.65
1965	32.52	36.61	34.57
1966	31.58	31.32	31.45
1967	31.91	32.56	32.24
1968	31.11	28.49	29.80
1969	30.95	27.55	29.25
1970	29.22	31.55	30.39
1971	28.70	32.58	30.64
1972	29.25	29.56	29.40
1973	34.59	33.64	34.11
1974	26.00	26.66	26.33
1975	30.13	30.61	30.37
1976	30.31	30.68	30.50
1977	27.88	35.08	31.48
1978	29.08	28.66	28.87
1979	26.44	27.09	26.77
1980	28.06	26.37	27.21
1981	28.94	28.63	28.78
1982	28.97	29.85	29.41
1983	29.51	29.61	29.56
1984	29.51	31.18	30.34

Table 3.2 $\delta^{18}O_{\alpha c}$ data for samples MZO30, MZO35, and the average $\delta^{18}O_{\alpha c}$ values of both samples.

	MZO30	**MZO35**	**Average**
$\delta^{18}O$ (‰) Value			
Lowest	21.04	23.68	24.5
Highest	34.59	36.61	34.57
Mean	28.85	29.78	29.32
Std. Deviation	2.62	3.08	2.46